N73-16485

STUDY OF THE DETAIL CONTENT OF APOLLO ORBITAL PHOTOGRAPHY

By: Robert E. Kinzly

CAL No. VT-2912-Ø-1

Prepared for:

Headquarters
National Aeronautics and Space
Administration
Washington, D.C.

FINAL REPORT
NSR-33-009-087
29 September 1972

CORNELL AERONAUTICAL LABORATORY, INC.
BUFFALO, NEW YORK 14221

CAL REPORT NO. VT-2912-0-1

STUDY OF THE DETAIL CONTENT OF APOLLO ORBITAL PHOTOGRAPHY

By: Robert E. Kinzly

FINAL REPORT

CONTRACT NO. NSR-33-009-087

29 SEPTEMBER 1972

Prepared by: *R.E. Kinzly, Head*
Optical Sciences Section

Approved by: *D.B. Dahm, Head*
Environmental Systems Department

Prepared for:

HEADQUARTERS
NATIONAL AERONAUTICS AND SPACE ADMINISTRATION
WASHINGTON, D.C.

ABSTRACT

This is the final report documenting the results achieved during a study of the Detail Content of Apollo Orbital Photography under Contract NSR-33-009-087 with NASA Headquarters. The study spanned a three year period and was composed of a series of tasks whose objectives were to assess the effect of residual motion smear or image reproduction processes upon the detail content of lunar surface imagery obtained from the orbiting Command Module. This report includes data and conclusions obtained from the Apollo 8, 12, 14 and 15 missions.

The specific tasks undertaken included (1) an evaluation of the residual motion smear present in Apollo 8, 12 and 14 photography, and (2) an assessment of the detail lost in reproduction of the original flight film for the Apollo 8, 12 and 15 missions.

For the Apollo 8, 12 and 14 missions, the bracket-mounted Hasselblad camera had no mechanism internal to the camera for motion compensation. If the motion of the Command Module were left totally uncompensated, these photographs would exhibit a ground smear varying from 12 to 27 meters depending upon the focal length of the lens and the exposure time. During the photographic sequences motion compensation was attempted by firing the attitude control system of the spacecraft at a rate to compensate for the motion relative to the lunar surface. The residual smear occurring in selected frames of imagery was assessed using edge analyses methods to obtain an achieved modulation transfer function (MTF) which was compared to a baseline MTF. The results in the case of the Apollo 8 analysis showed that 14-36% of the motion was compensated increasing the ground resolution to better than 20 meters. In the case of Apollo 12 and 14 photography the high solar elevation angles prevented an adequate assessment from being performed.

The original flight film from all of the Apollo orbital photography is reproduced for distribution to potential data users. The higher order generations produced by the reproduction process can suffer a loss of detail content. Therefore the second major task of the study was to determine if such a loss occurred. Two sources of degradation were assessed; a loss in resolution or fine detail as measured by the MTF of the copy compared to the original flight film and a loss in contrast as measured by the difference between the sensitometric calibration of the copies and flight film.

An evaluation of the loss in resolution was made for the Apollo 8, 12 and 15 missions. The results showed no significant loss occurred in any of the imagery evaluated.

The evaluation of loss in contrast was only made for the Apollo 15 imagery. In this case visual inspection of enlargements made by some of the users had indicated a softening of some detail particularly within shadowed and bright surface areas. Evaluation of the sensitometric data show a decrease in contrast for lunar surface features in bright and dark regions for both panoramic and metric camera imagery. This loss in contrast is produced by density compression of the toe and shoulder of the response curve for the reproduction process. To avoid this loss, film with a larger dynamic range must be employed or the chemistry adjusted to obtain a lower gamma.

The study successfully demonstrated the development and application of image evaluation techniques to orbital photography of the lunar surface. The results of the study were used to provide guidance in obtaining better detail content in successive Apollo missions. It also demonstrated that these techniques could be used in future manned and unmanned spacecraft involved in planetary exploration.

FOREWORD

The research reported herein is the result of a series of tasks performed over a three year period under Contract No. NSR-33-009-087 with NASA Headquarters and monitored by Mr. Leon Kosofsky (Code:MAL).

The author is grateful to Mr. Knol Lamar and Mr. Robert Hill of the NASA Manned Spacecraft Center for furnishing the Apollo Orbital imagery needed to perform the study, and to Mr. George Blackman also of the NASA Manned Spacecraft Center for the MTF data on flight-qualified lenses. In addition he wishes to acknowledge many helpful discussions with Mr. Douglas Lloyd of Belcomm, Inc. Contributions by others at Cornell Aeronautical Laboratory include Mr. Roger Haas for performing some of the microdensitometry and Mr. Melvin Mazurowski for assistance in processing the edge trace data.

TABLE OF CONTENTS

LIST OF FIGURES

LIST OF FIGURES (Cont.)

1. INTRODUCTION

This is the final report documenting the results achieved during a study of the Detail Content of Apollo Orbital Photography under Contract NSR-33-009-087 with NASA Headquarters. This study spanned a three year period and was composed of a series of tasks whose objectives were to assess the effect of residual motion smear or image reproduction processes upon the detail content of lunar surface imagery obtained from the orbiting Command Module. This report includes data and conclusions obtained from the Apollo 8, 12, 14 and 15 missions.

To meet the study objectives, analysis techniques which we had developed previously were extended and some new techniques developed. Consequently, the next section of this report will present a description of the methods and techniques used during the study. The remainder of the report describes specific tasks where these techniques were applied. These tasks included (1) an evaluation of the residual motion smear present in Apollo 8, 12 and 14 photography, and (2) an assessment of the detail lost in reproduction of the original flight film for the Apollo 8, 12 and 15 missions.

Before proceeding with the detailed discussion of the study it will be helpful to the reader if we review the photographic equipment used during the subject Apollo missions. Table 1 presents a summary of the cameras employed and their characteristics. The omission of some of the intermediate Apollo missions does not indicate that the cameras listed were not employed during these missions but only that the study did not involve a task dealing with the orbital photography from that mission. In the case of Apollo 13, of course, a spacecraft failure prevented the scheduled mission from being completed and no orbital photography was obtained.

Table 1

APOLLO ORBITAL PHOTOGRAPHIC CAMERAS

CAMERA	CHARACTERISTICS						APOLLO MISSION USED			
	FOCAL LENGTH (mm)	f-NUMBER	FILM TYPE	FRAME SIZE	GROUND RESOLUTION* (meters)	MOTION COMPENSATION	8	12	14	15
BRACKET MOUNTED HASSELBLAD	80 250 500	f/5.6 f/5.6 f/8	EK 3400 OR SO-164	70 mm	20** 27** 12***	PROVIDED THROUGH THE ATTITUDE CONTROL OF THE COMMAND MODULE	x x 	x x	 x	
LUNAR TOPO-GRAPHIC CAMERA (MODIFIED HYCON KA-74)	456 (18-inch)	F/4	EK 3400 AND EK 3414	4.5 x 4.5 inches	4	PROVIDED BY AUTOMATIC ROCKING OF THE CAMERA			x	
OPTICAL BAR PANORAMIC CAMERA (MODI-FIED ITEK KA-80A)	610 (24-inch)	f/3.5	EK 3414	5 x 45 inches	2	PROVIDED INTERNAL TO CAMERA				x
MAPPING CAMERA (FAIRCHILD)	76 (3 - inch)	f/4.5	EK 3400	4.5 x 4.5 inches	20	PROVIDED INTERNAL TO CAMERA				x

*AT A NOMINAL ORBITAL ALTITUDE OF 110 km.

**WITHOUT MOTION COMPENSATION AT AN EXPOSURE TIME OF 1/60 second.

***WITHOUT MOTION COMPENSATION AT AN EXPOSURE TIME OF 1/125 second.

For the Apollo 8, 12 and 14 missions, the bracket-mounted Hasselblad camera had no mechanism internal to the camera for motion compensation. If the motion of the Command Module were left totally uncompensated, these photographs would exhibit a ground smear varying from 12 to 27 meters depending upon the focal length of the lens and the exposure time. During the photographic sequences motion compensation was attempted by firing the attitude control system of the spacecraft at a rate to compensate for the motion relative to the lunar surface. The Command Module pilot used the Crew Optical Alignment Site (COAS) to view a fixed feature on the lunar surface and adjust the attitude control to keep that feature in the center of his field-of-view. If this technique were successful, then there would be no motion smear in the photography and its full potential could be achieved. One of the tasks in this study was to assess how much compensation was obtained using this technique during the Apollo 8, 12 and 14 missions. As can be seen from the table, the remainder of the cameras had internal motion compensation and consequently residual smear should not dominate the resolution of this photography.

The original flight film from all of the Apollo orbital photography is reproduced for distribution to potential data users. The higher order generations produced by the reproduction process can suffer a loss of detail content. Therefore the second major task of the study was to determine if such a loss occurred. Figure 1 shows the reproduction sequence and terminology used. For all the missions studied, a second generation or master positive (2P) copy was produced, copied to produce a third generation negative (3N) and copied again to generate a fourth generation positive (4P) copy. A few of the users receive master positives (2P) but most are likely to receive the fourth generation positive (4P) copy. An assessment of the effect of the reproduction sequence upon the image detail content was made for the Apollo 8, 12, and 15 missions.

The study successfully demonstrated the development and application of image evaluation techniques to orbital photography of the lunar surface. The results of the study were used to provide guidance in obtaining better detail content in successive Apollo missions. It also demonstrated that these techniques could be used in future manned and unmanned spacecraft involved in planetary exploration.

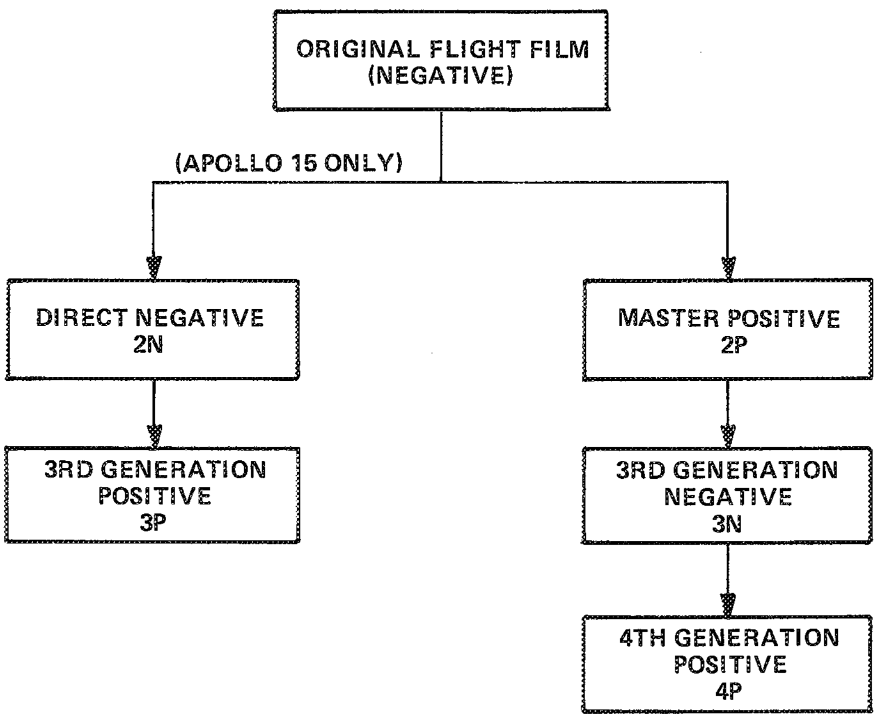

Figure 1 APOLLO ORBITAL PHOTOGRAPHY REPRODUCTION SEQUENCE

2. EVALUATION TECHNIQUES

Many of the methods used in the evaluation of the quality of the Apollo orbital photography were developed and demonstrated during a study of Lunar Orbiter image quality.[1]

The evaluation of the quality of Apollo Orbital photography can require the measurement of various properties of the imagery. The properties which define image quality can be divided into four general categories: (1) "resolution" or fine detail content, (2) contrast or tone quality, (3) noise level and (4) metric quality. Overall performance can be based upon a composite measure which includes several (or all) of the categories but must be determined with the intended use of the imagery in mind.

The modulation transfer function (MTF) is often used as a measure of image resolution or fine detail content. The MTF is used in this study to assess the amount of uncompensated image motion present in the photography. To accomplish this one must have a baseline MTF (no image motion smear) to compare to the achieved or operational MTF. Both the achieved and baseline MTF's were evaluated using microdensitometry of selected test targets such as tri-bar charts and sharp edges. The procedures developed to obtain this data are described in this section of the report. Comparison of MTF's was also used to determine the loss of fine detail during the reproduction sequence.

Contrast or tonal quality can best be described as the fluctuation in density due to large area intensity differences in the scene (i.e., fluctuations observed when the photograph is scanned with an aperture which is large compared to the smallest resolved detail). Such fluctuations are used by the photoanalysist to classify objects or delineate boundaries. The most common measure of tonal quality is the Hurter-Driffield or D-Log E response curve for the image. It describes how scene brightness is reproduced as density in the image. The D-Log E response curve for the original flight film was compared to that for the higher generations (copies) to evaluate the tonal quality and its effect on detail content.

During the study we did not find it necessary to evaluate the quality in the last two categories (noise level and metric quality) in order to assess the detail content relative to the intended use of the imagery.

2.1 <u>Frame Selection and Estimating Motion Smear.</u> - In selecting the actual frames to be evaluated consideration was given to two areas; (1) the availability of test targets, particularly shadow-to-sunlight edges inside craters, for estimating the achieved MTF and (2) selecting those which would have the largest amount of motion smear if no compensation were attained.

The application of edge analysis techniques to imagery of the lunar surface for the evaluation of the camera system MTF has been developed and conclusively demonstrated in an earlier study of the Lunar Orbiter imaging system(1). This technique involves the use of a microdensitometer to scan several shadow-to-sunlight edges in craters near the principal point in the photographic format. The availability and suitability of the edges depends upon the solar elevation angle at which the lunar photography was taken. At high sun angles an edge will not exist and at extremely low sun angles the edge will be sufficiently close to the far rim of the crater to make edge analysis impractical. Assuming that the shape of the crater can be reasonably represented by a spherical model the ratio of the length of a shadow, L, to the diameter of the crater, D, can be expressed in terms of the diameter-to-depth ratio, r, and solar elevation angle, θ, namely

$$\frac{L}{D} = \cos^2\theta - \frac{r^2-4}{8r} \sin 2\theta \qquad (1)$$

By letting $L = 0$, we can determine the maximum value of solar elevation angle which will produce a shadow-to-sunlight edge interior in the crater. The maximum angle as a function of crater diameter-to-depth ratio is shown in Table 2. As the solar elevation angle approaches this limit the shadow-to-sunlight edge approaches the near rim of the crater making the use of edge techniques impractical. The shadow length should be several resolution elements so that the image of the rim does not interfere with the shadow-to-sunlight edge.

Table 2
MAXIMUM PERMITTED SOLAR ELEVATION ANGLES FOR SHADOW-TO-SUNLIGHT EDGES

CRATER DIAMETER-TO-DEPTH RATIO	MAXIMUM SOLAR ELEVATION
5	44°
6	37°
7	32°
8	28°
9	25°
10	22.5°

In addition to the availability of targets, the second consideration in the case of the Apollo 8, 12 and 14 missions involves maximizing the magnitude of the blur in the image if the motion were left totally uncompensated. The measurement of the amount of compensation is easier in those frames with the largest amount of potential blur. The most vertical frames of photography would have the greatest amount of smear if the motion were left totally uncompensated. The distance between two separated landmarks occurring on each frame in the sequence under consideration was measured in order to estimate the tilt angle from the vertical for each frame. The frame having the largest separation is the most vertical frame. By combining these data with the altitude and velocity of the command module, we computed the blur expected in each of the frames if no compensation were achieved.

The magnitude of the blur at the lunar surface is not equal to the product of the velocity of the Command Module and the exposure time. Figure 2 shows the geometry for vertical and oblique photographic frames. The expression for the blur b is

$$b = \frac{Vt_e}{1 + h/r_m} \tag{2}$$

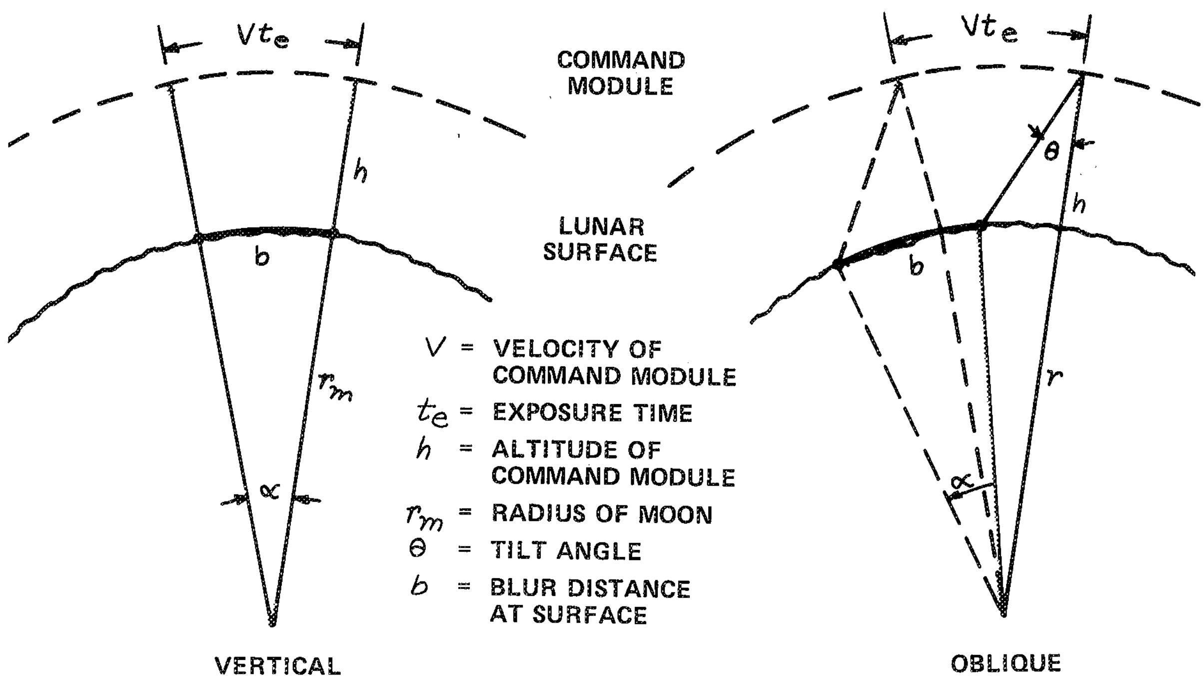

Figure 2 MAGNITUDE OF MOTION SMEAR AT THE LUNAR SURFACE

In order to convert this blur on the surface to an equivalent angular blur we simply divide by the altitude in the case of the vertical photograph. For the oblique photograph two additional effects must be included; the foreshortening of b due to the tilt angle and the increase in distance between the camera and the principal ground point (center of the image). The resulting expression for the angular blur, $\delta\alpha$, are

$$\delta\alpha = \frac{V}{h} \frac{1}{[1+h/r_m]} t_e \qquad \text{(vertical)} \qquad (3a)$$

$$\delta\alpha = \frac{V}{h} \frac{\cos^2\theta}{[1+h/r_m]} t_e \qquad \text{(oblique)} \qquad (3b)$$

We see that the effective angular rate (obtained by dividing by t_e) is less than V/h in both bases.

In order to compute the blur for the photography obtained with the bracket-mounted Hasselblad camera, the measured distance between two separated landmarks is combined with the nominal altitude of the Command Module and the focal length of the lens to compute slant range, tilt angle and blur magnitude for each photographic frame in the selected sequence. The expression used to compute the tilt angle is

$$\theta = \cos^{-1}\left\{\frac{h^2 + 2hr_m + R_s^2}{2R_s(h+r_m)}\right\} \qquad (4)$$

where R_s = slant range to principal point and h and r_m are as defined previously in Figure 2.

These techniques were applied to the assessment of residual motion smear in Apollo 8, 12 and 14 photography; the results are presented in later sections of the report.

2.2 Calculating MTF from Tri-Bar Charts. - It is customary to represent the degradation of a noiseless image in an optical system by using a function called the modulation transfer function (MTF). This function is the Fourier transform of the image of a point object. Generally, the image of a point object is degraded or spread, causing degradations expressed by the modulation transfer function. The MTF can be measured for a system by photographing test charts that have a sinusoidal variation in illuminance. The maximum and minimum density levels of the sinusoidal image are measured using a microdensitometer, converted to exposure values and used to compute the modulation of the image, viz.

$$M_i(\nu) = \frac{E_{max} - E_{min}}{E_{max} + E_{min}} \tag{5}$$

where ν is the spatial frequency of the sinusoidal target. This modulation is then divided by the initial, known modulation of sinusoidal test target, $M_o(\nu)$, to determine the MTF,

$$\tau(\nu) = \frac{M_i(\nu)}{M_o(\nu)} \tag{6}$$

Another type of test target that can be used to determine the MTF is the tri-bar chart. In this case the target contains higher harmonics of the fundamental spatial frequency (i. e. reciprocal of the bar spacing) and more complex processing must be employed to obtain the MTF. Again we use a microdensitometer to measure the modulation of the test target image. The procedure for converting the measured square-wave response, $R(\nu)$, to the corresponding sine wave response or MTF is based upon an expression developed by Coltman(2) and given by,

$$\tau(\nu) = \frac{\pi}{4M_o}\left\{R(\nu) + \frac{R(3\nu)}{3} - \frac{R(5\nu)}{5} + \cdots\right\} \tag{7}$$

Again the initial modulation of the test chart must be known in advance.

If the initial modulation is not known we developed a procedure for estimating the modulation at zero spatial frequency. This procedure is based upon results presented by Charman(3). He has computed the modulation of two-bar, three-bar, square-wave and sine-wave targets for a diffraction-limited optical system. The equivalent three-bar, square-wave (infinite number of bars) and sine-wave modulations are shown in Figure 3.

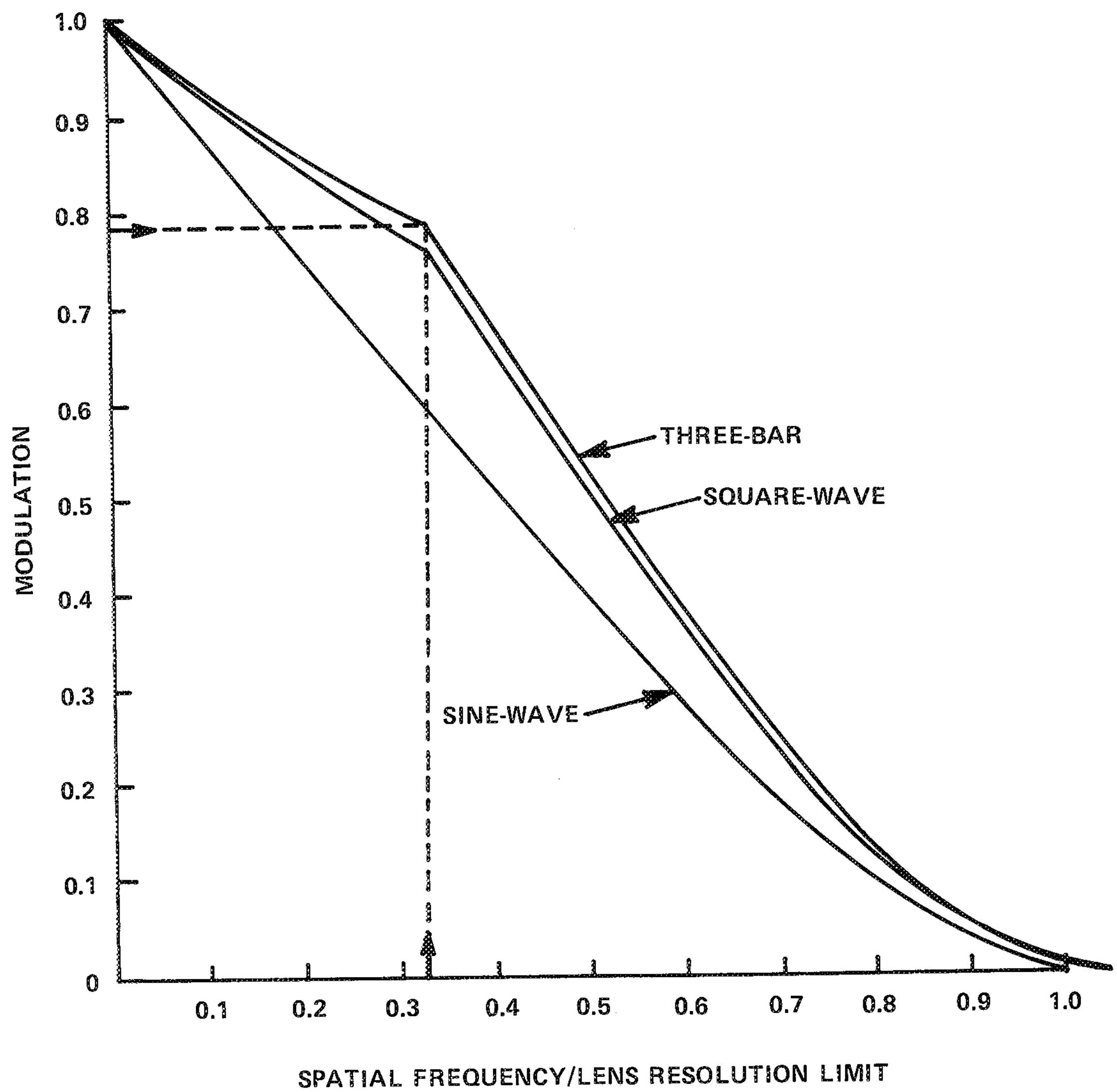

Figure 3 MODULATION OF SEVERAL RESOLUTION TARGETS FOR A DIFFRACTION-LIMITED LENS

Note that the sine-wave modulation shows a smooth transition between zero spatial frequency and the resolution limit; whereas the two-bar, three-bar and square-wave targets show a characteristic discontinuity in the modulation occurring at one third of the resolution limit. The measured response at this discontinuity for the three-bar target is equal to 0.78 times the modulation at zero frequency. Thus we found that this modulation, M_0, can be estimated by using the following procedure: (1) an estimate of the resolution of the imaging system is obtained by noting the spatial frequency at which the square wave drops to 5 to 10 percent of the initial modulation, (2) the modulation at one third of the resolution limit is divided by 0.78 to estimate M_0.

In most cases manufacturers were not required to furnish camera MTF data which we could have used to establish baseline performance. Usually, however, NASA photographed an NBS Resolution Chart onto the leader of the flight film prior to launch. The technique described above was used to obtain baseline performance from the NBS chart image in the assessment of residual motion smear.

2.3 Calculating MTF from Edge Traces. - In many cases sine-wave or tri-bar test charts are not provided with photographs, thus the MTF must be determined in another way. In practice, the mathematical relation of the line spread to the microdensitometer trace of an edge image is used to obtain the MTF.

To accomplish this we previously developed a procedure to scan a naturally occurring sharp edge in the image format using a rectangular or slit aperture in the microdensitometer. The edge data is sampled, smoothed to reduce the noise, and converted to digital form for computer analysis. This smoothed edge density trace is converted to exposure (illuminance trace) and differentiated to determine the line spread function

L(x). The modulation transfer function $\tau(\nu)$, is calculated from the expression

$$\tau(\nu) = \int L(x)\, e^{2\pi i \nu x}\, dx$$

i.e., the Fourier transform of the line spread.

A more detailed description of the data flow in this process is shown in Figure 4. Since the edge traces obtained from the microdensitometer

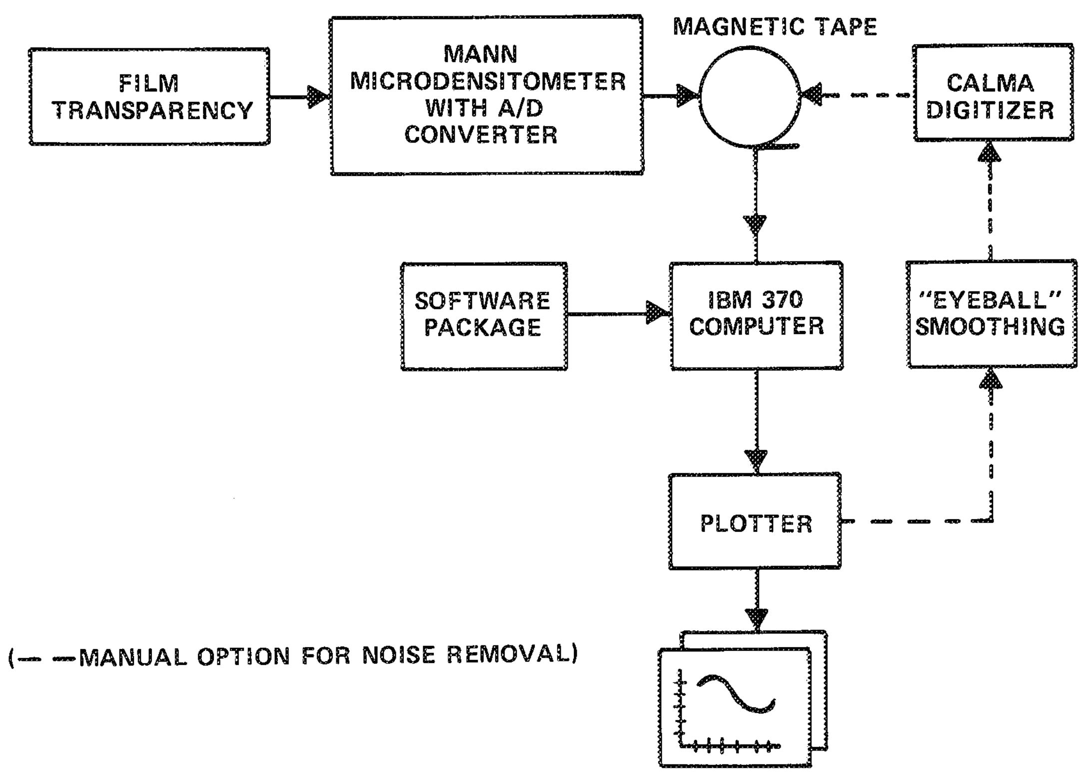

Figure 4 DATA FLOW FOR MTF DETERMINATION FROM EDGE TRACES

contain noise (due to film grain if nothing else) they must be smoothed or some statistical procedure employed in estimating the MTF. Our software package contains a number of options including non-stationary filtering in both spatial and frequency space, modulus averaging and complex averaging. The later two techniques require that traces of several edges be obtained from the image under evaluation. Several shadow-to-sunlight edges occurring inside craters within the image format were scanned using our microdensitometer and the modulus averaging technique used to obtain the operational MTF for the assessment of residual motion smear and the fine detail degradation of the reproduction sequence. In some of our previous work the MTF was used as a diagnostic tool for assessment of residual motion blur[4, 5].

2.4 Establishing Baseline Performance. - In the case of the bracket mounted Hasselblad camera the modulation transfer function measured from the edge traces will represent the product of the inherent modulation transfer function of the camera system multiplied by the transfer function representing the additional degradation due to uncompensated motion smear. If the baseline performance or MTF is known then a residual MTF due to smear can be determined from the achieved MTF by a simple process of division. Unfortunately, no modulation transfer function data are available for any of the lenses used with the Hasselbald camera during the Apollo missions. Even if such data were available it would not include the degrading influence of the original (flight) film used in the camera system or the contact printing process used to reproduce higher generation copies from which some of our measurements were made. These additional degradations are part of the baseline performance since they influence the detailed content of the photography even if all the motion smear were removed.

In order to evaluate the baseline performance, we estimated the modulation transfer function using data obtained by measuring the high contrast NBS resolution charts photographed through the 80mm focal length lens onto the leading edge of the film prior to each mission. Although it would have been preferable to make such measurements from resolution charts imaged through the 250mm or 500mm focal length lenses, none were available.

Measurements were made by Mr. George Blackman of the Mapping Sciences Laboratory at the NASA Manned Spacecraft Center of the modulation transfer functions of several flight-qualified lenses. Thus the data obtained by measuring the high contrast NBS resolution charts can be corrected to account for the differences between the 80mm focal length lens and the lens used to obtain the photography being analyzed. An average on-axis lens MTF was determined from several individual measurements supplied by Mr. Blackman and the results are presented in Figure 5. It is easily seen that the performance of these lenses vary considerably.

By dividing the MTF of the longer focal length lens by the 80mm lens MTF the correction required to account for the differences between the lenses was obtained and is shown in Figure 6. These correction functions were subsequently used to compute baseline performance for the 250mm lens on Apollo 8 and the 500mm lenses on Apollo 12 and 14.

In addition to being useful in the determination of baseline performance the measurements of lens MTF also permit a comparison of the relative merits for selecting between the various focal length lenses. The advantage of magnification obtained by employing longer focal lenses is only significant if in the design of the various lenses and attempt is made to match the modulation transfer functions as nearly as possible. As the focal length becomes longer it becomes increasingly difficult to maintain the same modulation transfer function or resolution at the image plane scale. Examining the data presented in Figure 5 we clearly see that the average performance at the image plane decreases for increasing focal length. Consequently part of

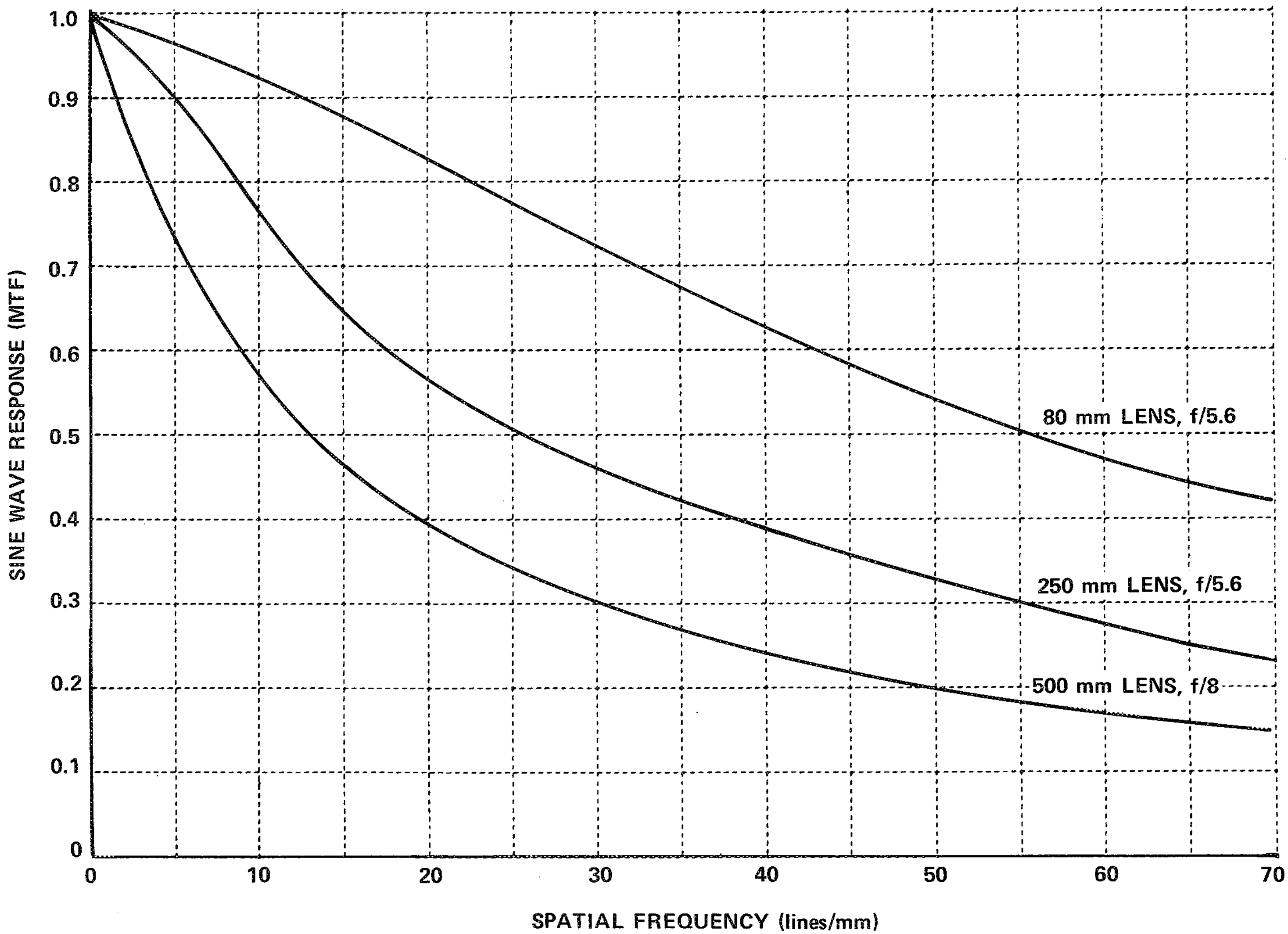

Figure 5 AVERAGE MEASURED LENS MTF (MAPPING SCIENCES LABORATORY/MSC)

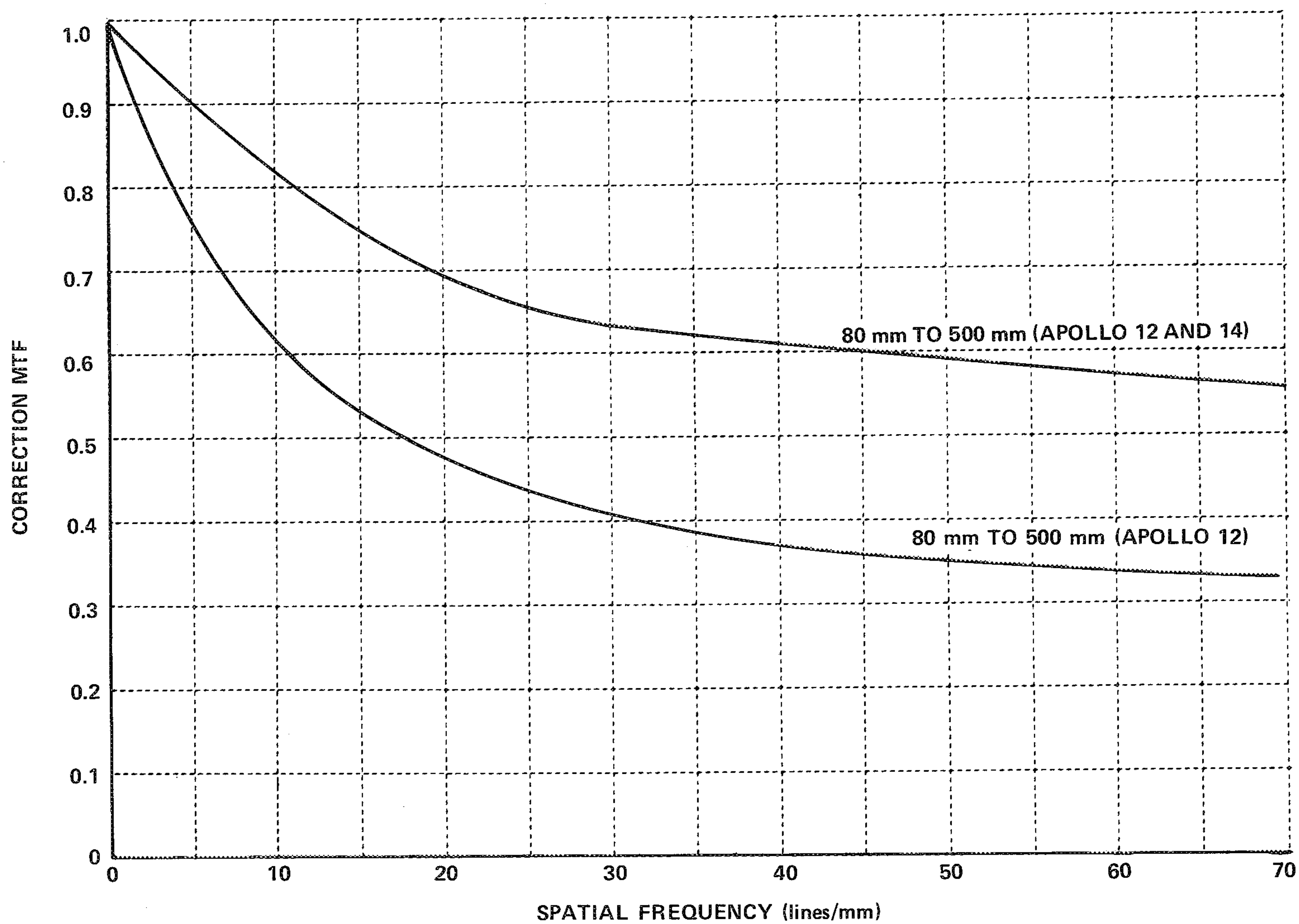

Figure 6 CORRECTION MTF REQUIRED TO ESTABLISH BASELINE MTF

the magnification obtained by increasing the focal length is empty and will not yield increased ground resolution. This becomes clearer if we scale the spatial frequency in the image plane by the focal length of the lens and plot the modulation transfer function in terms of the product of spatial frequency and the lens focal length (normalized frequency). This plot (Figure 7) clearly indicates that the response of the 250mm lens and the 500 mm lens are both better than the 80mm lens but the two longer focal length lens appear to be equivalent. There is some indication that a higher response exists at higher frequencies for the 500mm lens indicating that it would have an increased resolving capability for high contrast objects. However, unless lunar photography is being taken at very low sun elevation angles (near terminator photography) this increase in high contrast resolution will not be realized in the imagery. If we include the effects of noise in the image (that is film granularity), lunar features near the ground resolution limit should be more easily seen in the 500mm imagery. Since the image occupies an area four times larger than the 250mm image and the noise power is inversely proportioned to the square root of the area, the 500mm imagery has a better signal-to-noise ratio. However, in view of the large decrease in areal coverage from the 500mm (a factor of 4), the 250mm focal length would yield more information. We also should mention the variability in the performance between the 250mm lenses (2σ the deviation about the average) was computed to be 0.09. In the case of the other lenses an insufficient number were tested to evaluate the deviation.

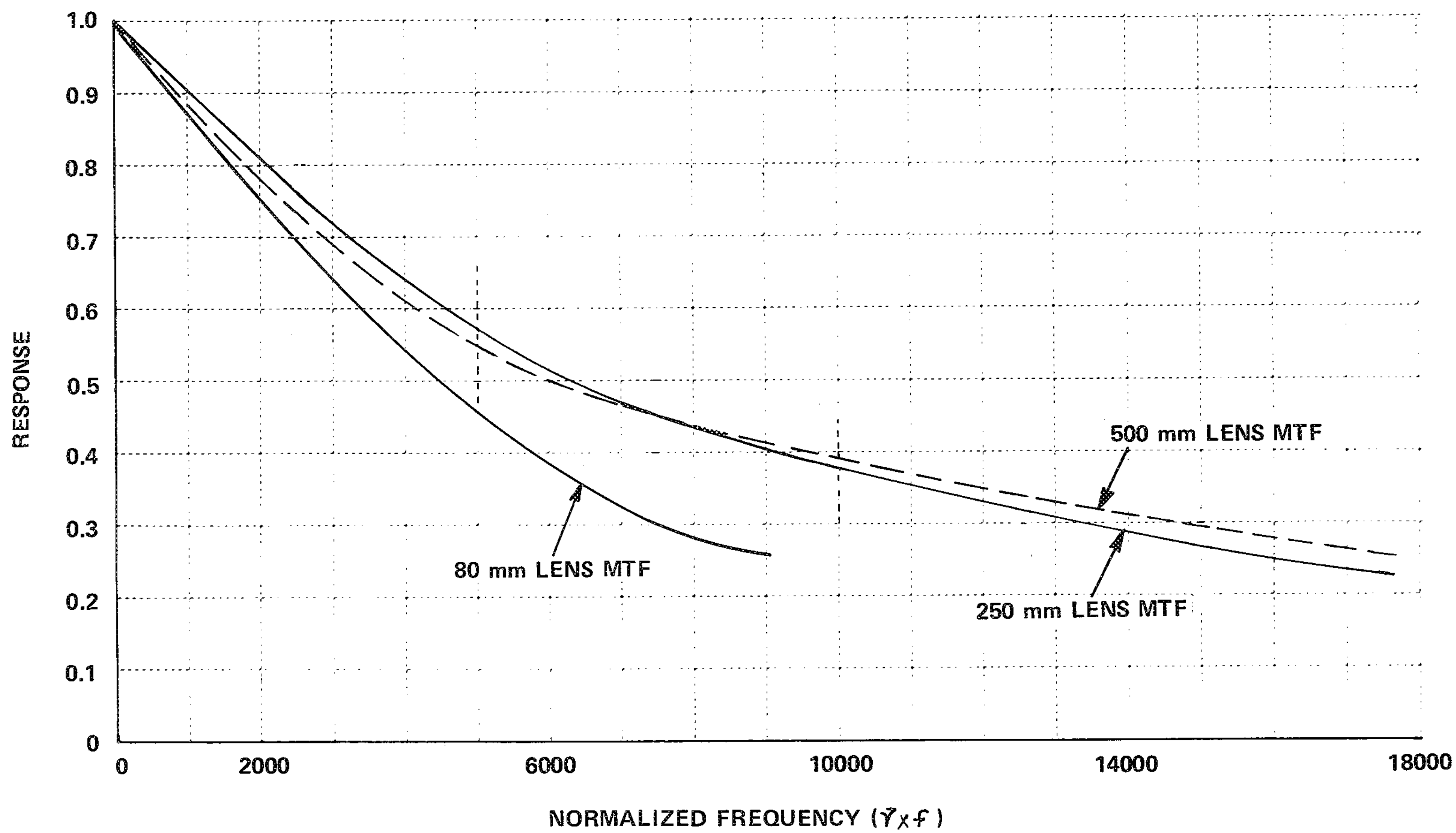

Figure 7 COMPARISON OF THE AVERAGE RESOLVING CAPABILITIES OF THE 80mm, 250mm AND 500mm FOCAL LENGTH LENSES USED WITH HASSELBLAD CAMERAS

3. ASSESSMENT OF RESIDUAL MOTION SMEAR

Three tasks were undertaken to assess the residual motion smear present in the bracket-mounted Hasselblad photography acquired on Apollo 8, 12 and 14 missions. Motion compensation was provided by using the Command Module attitude control system combined with visual tracking by the CM pilot. On Apollo 8 the 250mm lens was employed with an exposure time of 1/60 of a second while the 500mm lens was used with an exposure time of 1/125 of a second on Apollo 12 and 14. The uncompensated blur on the lunar surface is 27 meters and 12 meters, respectively.

A sequence of 10 photographs (frame 2300 through frame 2309) were taken during the Apollo 8 mission. In order to assess how much compensation was obtained, edge analysis techniques were applied to the subject photography. The frames representing the most nearly vertical photography were selected from the sequence of ten photographs using the procedure described in Section 2.1. These frames would have the largest amount of motion smear if left totally uncompensated. Edges were scanned with a microdensitometer using a second generation positive transparency furnished by U. S. Geological Survey, Flagstaff, Arizona. The edge exposure function, however, undergoes the non-linear transform during photographic recording resulting in a density or transmittance function on the film transparency. Such non-linear transformations distort the harmonic content of the images and one must convert the measured density or transmittance edge function into an exposure function in order to accurately determine the MTF. Only in those cases where the exposure difference across the edge is small can the correction for the non-linear response be neglected. In the present study the edges chosen for analyses are the shadow-to-sunlight edge interior to the craters which vary over a large range in exposure. Fortunately, several sets of sensitometric calibration data were provided on the leading edge of the film allowing the

Hurter-Driffield curve or non-linear response to be measured. The response curve for the Apollo 8 2P copy (Magazine E) is presented in Figure 8 and shows excellent agreement between the individual sources of data. Similar sensitometric calibration curves were generated for the Apollo 8 flight film (Figure 9); Apollo 12 flight film (Figure 10) and 2P copy (Figure 11) as well as an Apollo 14 4P copy (Figure 12).

The tilt angles computed for the Apollo 8 photographic sequence are shown in Table 3. Clearly the sequence began after the Command Module

Table 3
TILT ANGLES FOR THE APOLLO 8 SEQUENCE

FRAME NO.	TILT ANGLE (degrees)
2300	22.6
2301	23.8
2302	34.1
2303	38.7
2304	44.1
2305	44.5
2306	55.3
2307	58.9
2308	62.0
2309	64.5

had passed the vertical location. Consequently frames 2300 through 2304 inclusive and frame 2307 were selected for assessment. Although the exact sun elevation angle was not known, all of the photographs had distinct shadow-to-sunlight edges inside craters.

Three sequences of possible interest were identified by the sponsor within the Apollo 12 mission. The first sequence (Descartes) includes frames

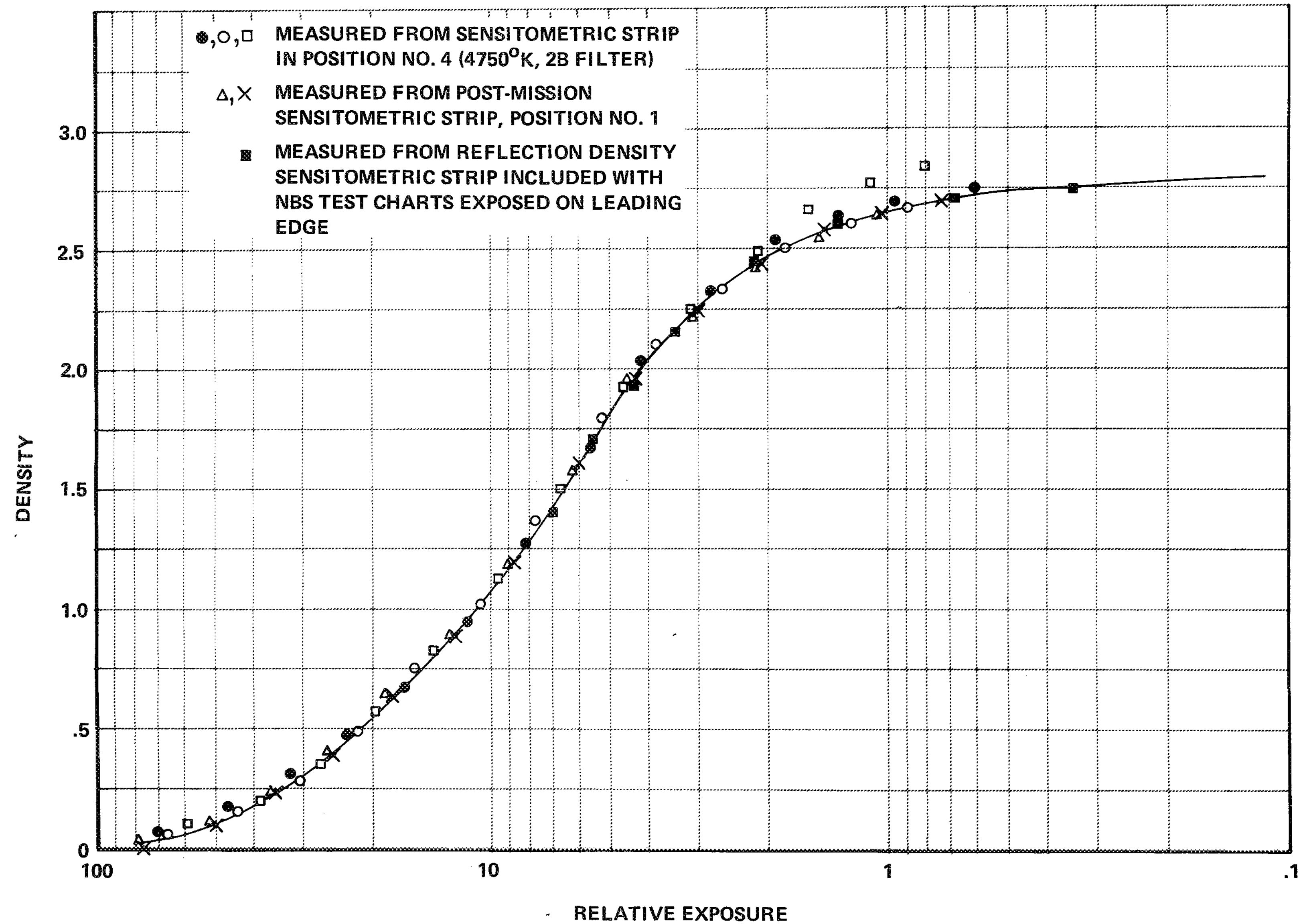

Figure 8 SENSITOMETRIC CALIBRATION – APOLLO 8 2P COPY (MAG. E)

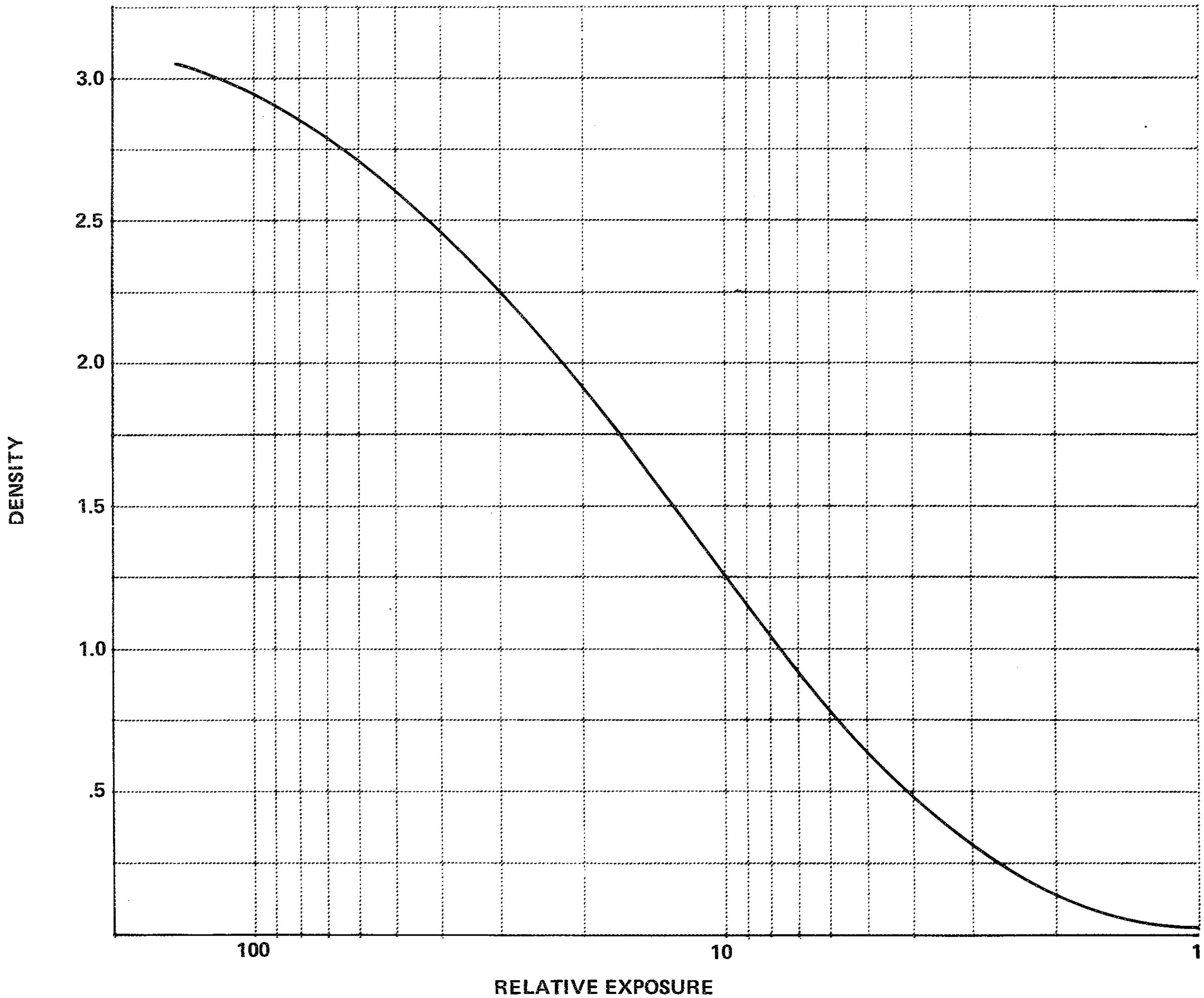

Figure 9 SENSITOMETRIC CALIBRATION – APOLLO 8, FLIGHT FILM (MAG. U)

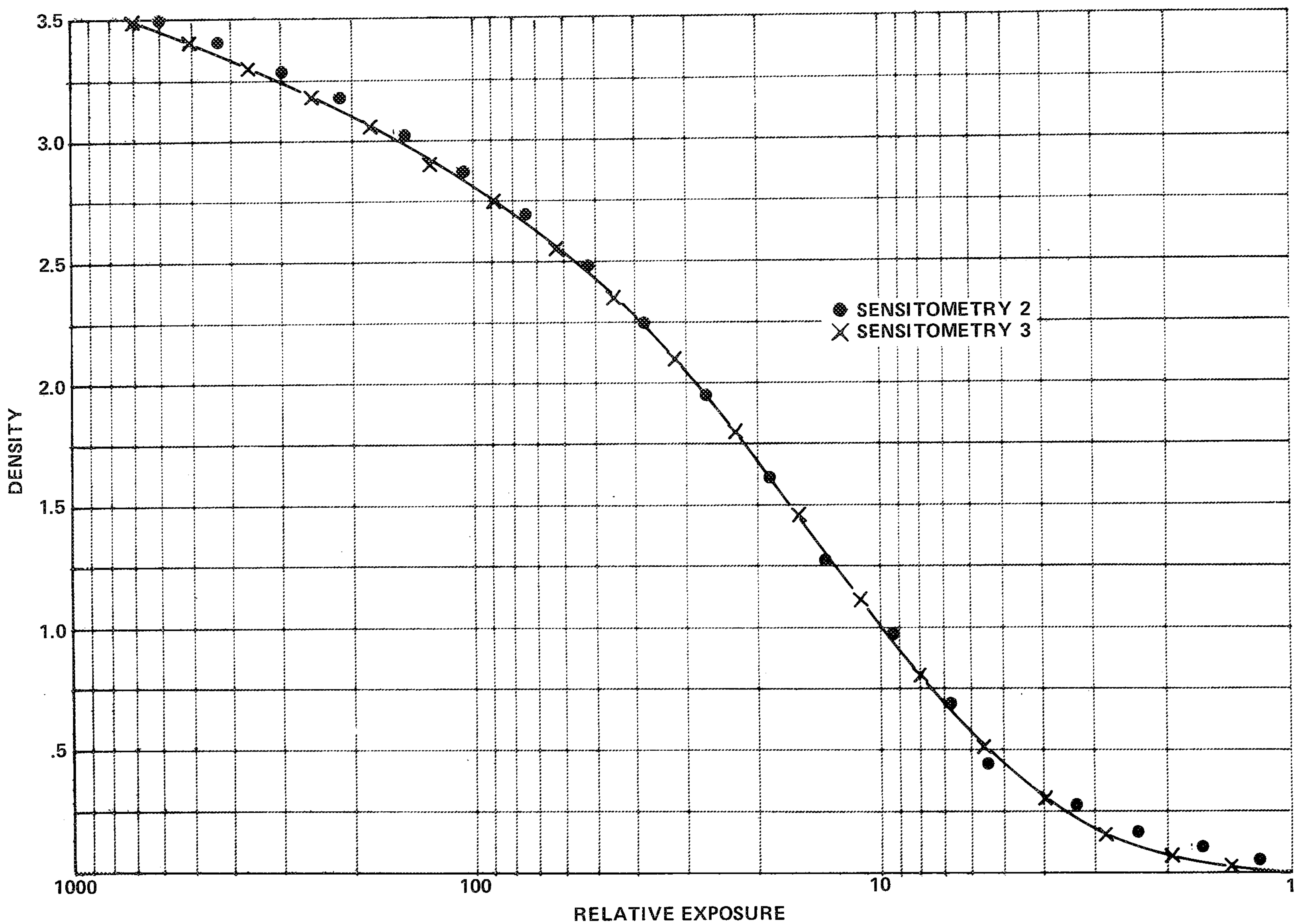

Figure 10 SENSITOMETRIC CALIBRATION – APOLLO 12, FLIGHT FILM (MAG. U)

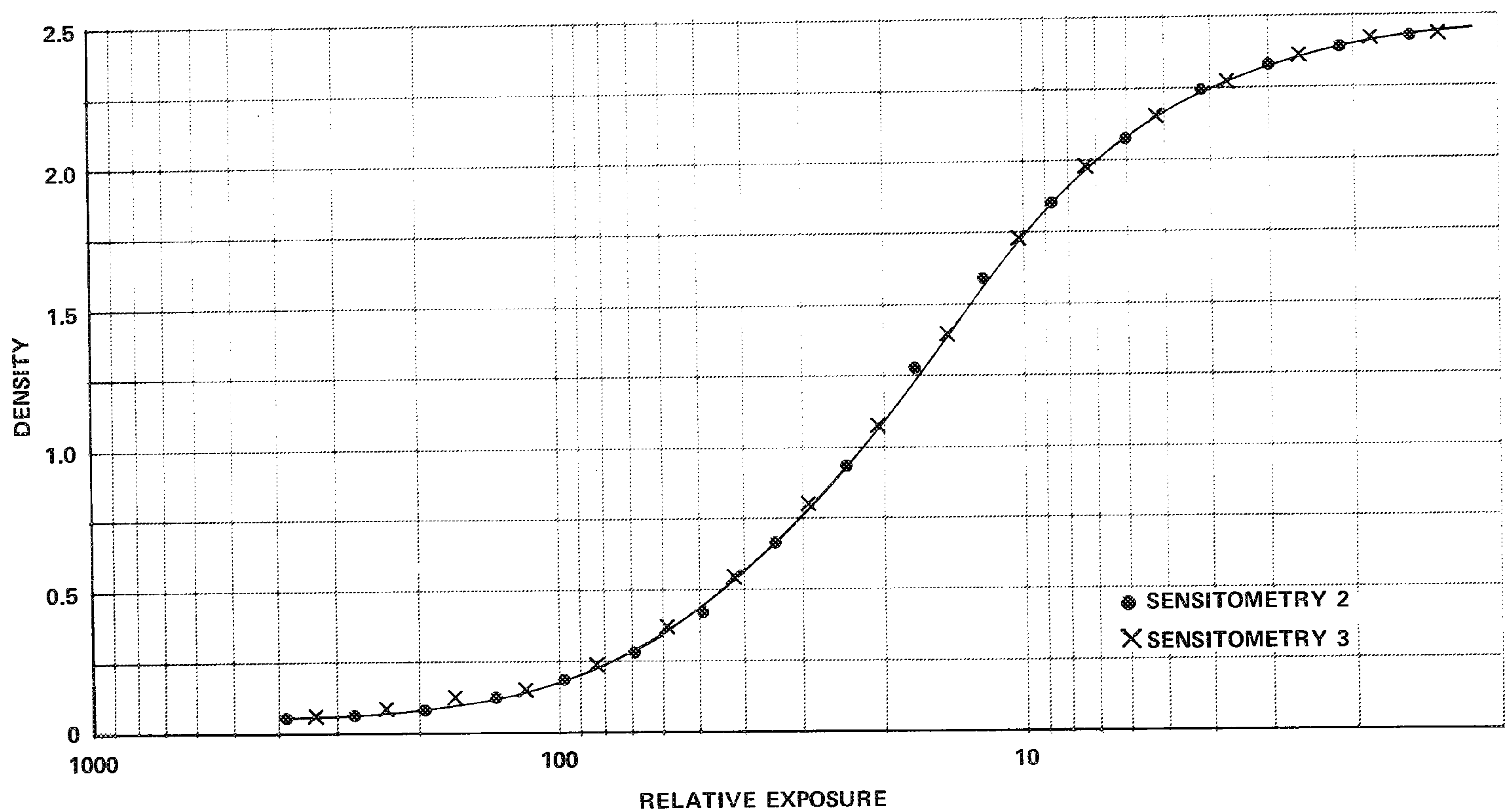

Figure 11 SENSITOMETRIC CALIBRATION – APOLLO 12 2P COPY (MAG. U)

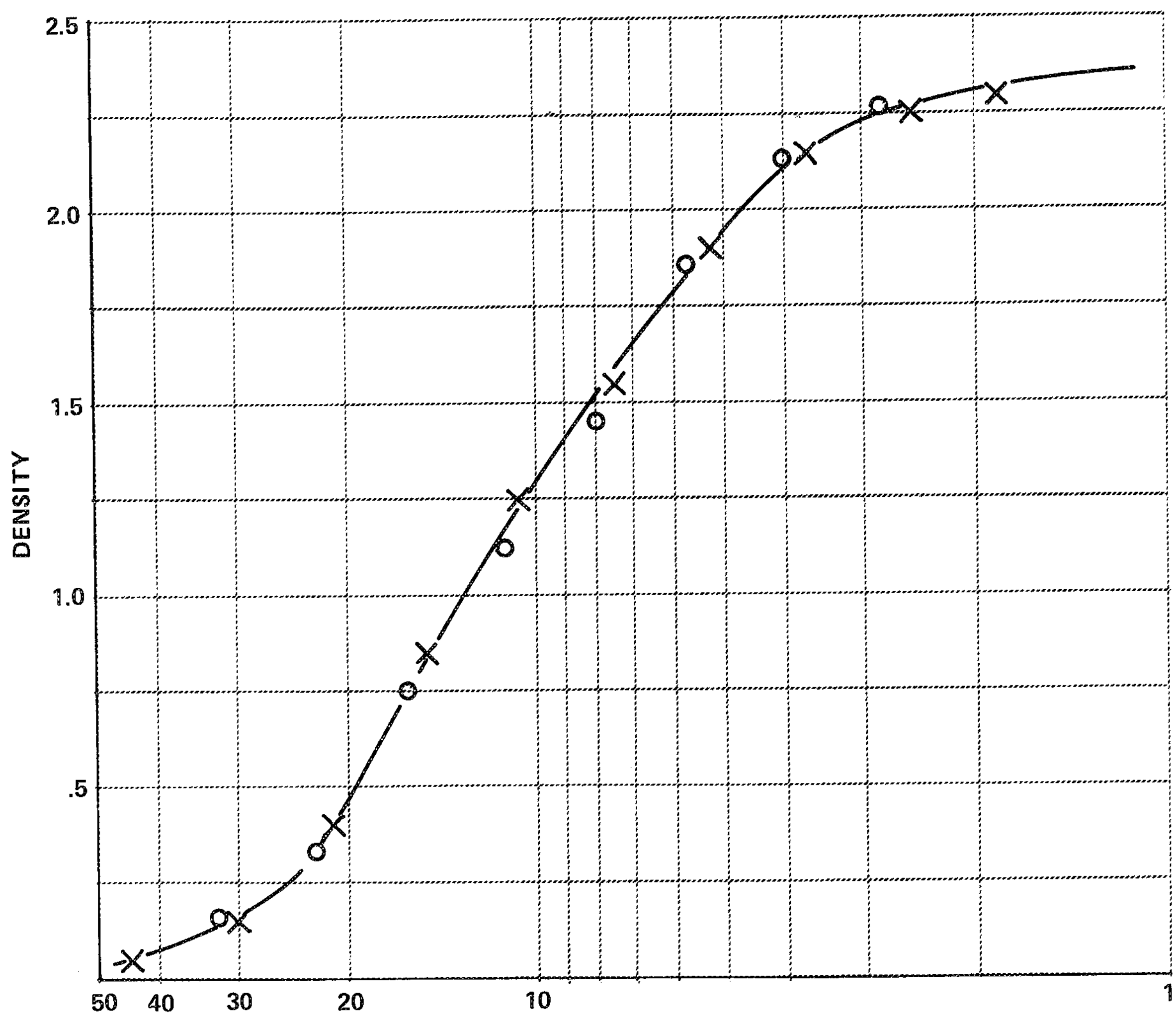

Figure 12 SENSITOMETRIC CALIBRATION – APOLLO 14 4P COPY (MAG. P)

7763 through 7803; the second sequence (Fra Mauro) includes frames 7804 through 7844; and the third sequence (LaLande) includes frames 7845 through 7886. All of these frames were taken at an exposure time of 1/125 of a second through the 500mm focal-length lens. Table 4 shows the seen elevation

Table 4

SOLAR ELEVATION ANGLES FOR THE APOLLO 12 SEQUENCES

SITE	SUN ANGLE (degrees)
FRA MAURO	38^o
LA LANDE	47^o
DESCARTES	71^o

angles for each of the sequences. Comparing these angles with the limits shown in Table 2 we can conclude that it is highly unlikely that shadow-to-sunlight edges inside craters will be available for the sequences of photography taken at the Descartes and LaLande sites. In the case of the Fra Mauro site, shadows are only likely to occur in very deep craters or in surfaces tipped away from the sun. Thus the procedure presented in Section 2.1 was only used to compute the tilt angle for the Fra Mauro site sequence. The results are shown in Figure 13. The numbers in brackets indicate the magntiude of blur at the film plane in microns if the motion were left totally uncompensated. Because of the possible lack of targets due to the high solar elevation angle only frames 7833 and 7834 were selected for evaluation.

The photographic sequences of interest during the Apollo 14 mission were taken near Descartes and have solar elevation angles of 58 degrees. Consequently, they do not contain any shadow-to-sunlight edges. The tilt angles for the photography in one of the sequences are presented in Table 5.

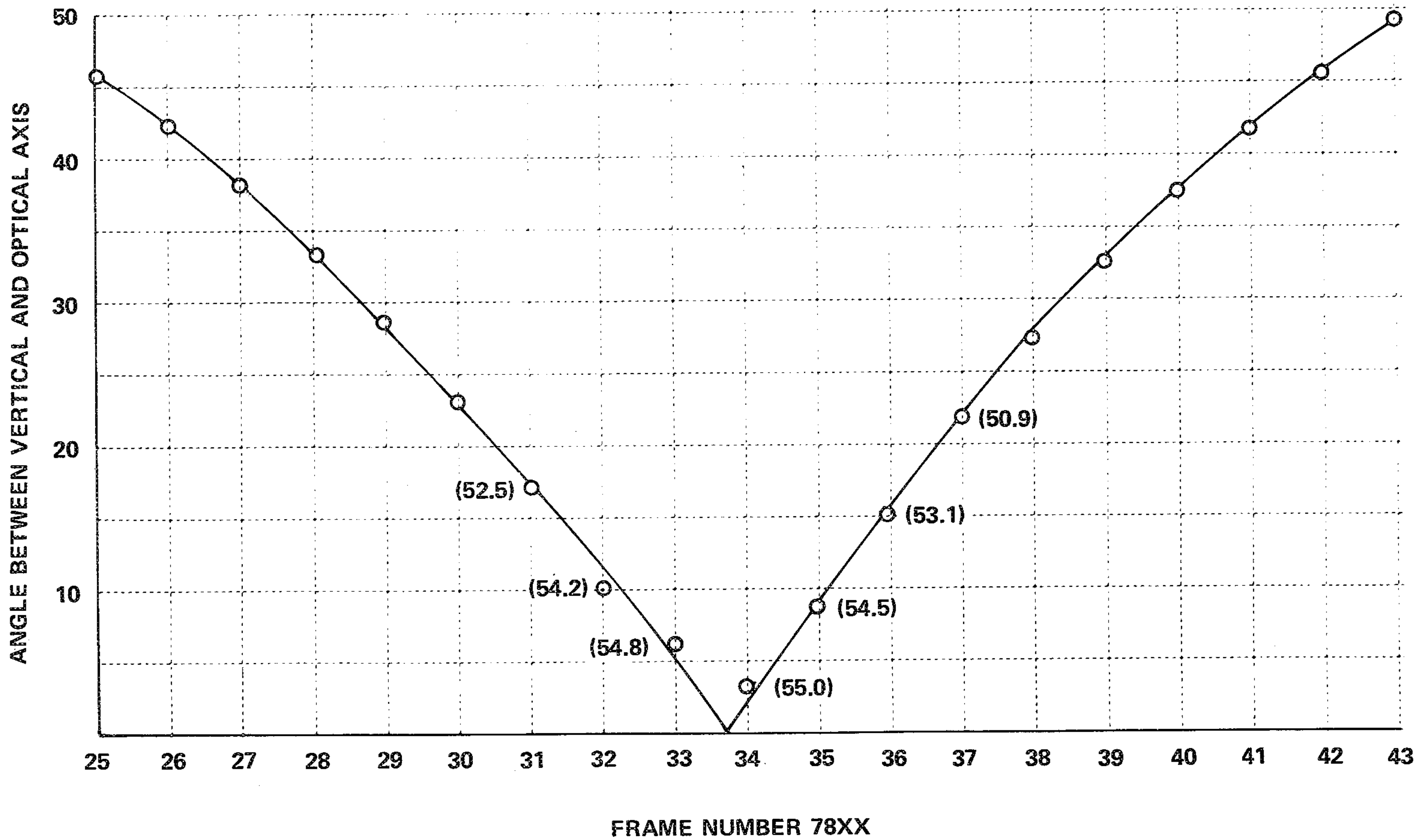

Figure 13 CAMERA TILT ANGLE – APOLLO 12, FRA MAURO SEQUENCE

Table 5
TILT ANGLES FOR THE APOLLO 14 SEQUENCE

FRAME NO.	TILT ANGLE (degrees)
9517	18.1
9518	16.3
9519	8.9
9520	4.3
9521	4.3
9522	11.9
9523	14.3
9524	18.1

In order to evaluate the Apollo 12 and Apollo 14 sequences other targets were sought which would be amenable for MTF evaluation. During our study of Lunar Orbiter photographic quality[(1)] most other sources were judged to be too subject to variation. On Apollo 12 deep craters or those sloped away from the sun were sought and several such targets were thought to be found. On Apollo 14 such targets did not occur, however, an apparently sharp edge of a bright ray was located as shown in Figure 14.

The methods described in Sections 2.2 and 2.4 were used to evaluate the baseline performance for all three missions. The results obtained are presented in Figure 15. Note that the baseline performance of the two 500mm lenses is in close agreement as would be expected.

Although NASA did not obtain a complete MTF for each of the lenses furnished it did require the manufacture to measure the response to a 20 cycle/mm sine wave at several format positions. The on-axis measurement of a 250mm lens and a 500mm lens are included in Figure 15 for reference. We

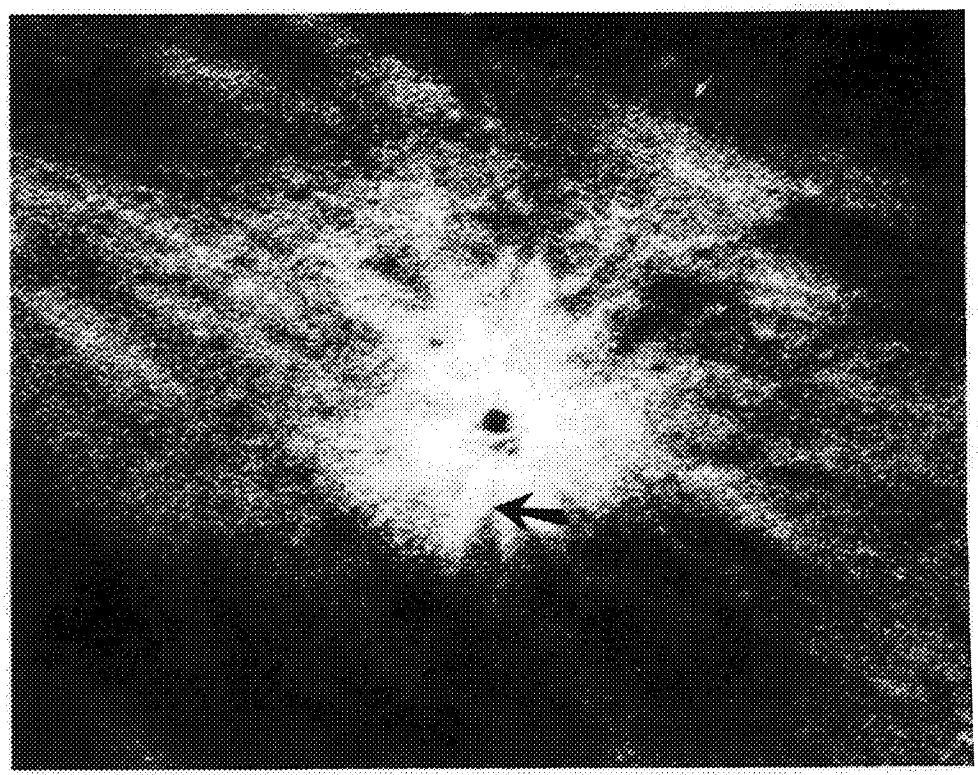

Figure 14 EDGE OF RAY USED FOR EVALUATION OF APOLLO 14 ORBITAL PHOTOGRAPHY (HASSELBLAD-500 mm LENS)

should include the degradation of the film (EK 3400) in which case the points would be lowered to about 75% of the value shown and would bring the data into reasonable agreement. This was not done to allow the reader to judge the contribution of the film response to the baseline performance.

The next step in the assessment is the measurement of the achieved MTF using shadow-to-sunlight edges for Apollo 8 and 12 and the ray for Apollo 14. In each frame 10 - 15 craters were selected near the center of the format and the shadow-to-sunlight edge in their interior scanned with a 1 by 34 micron slit. An observer fit a smooth curve through each of the resulting density traces and these smooth curves were digitized for processing on a computer. The processing involves converting the smooth density traces to an edge exposure function using the sensitometric curve described earlier.

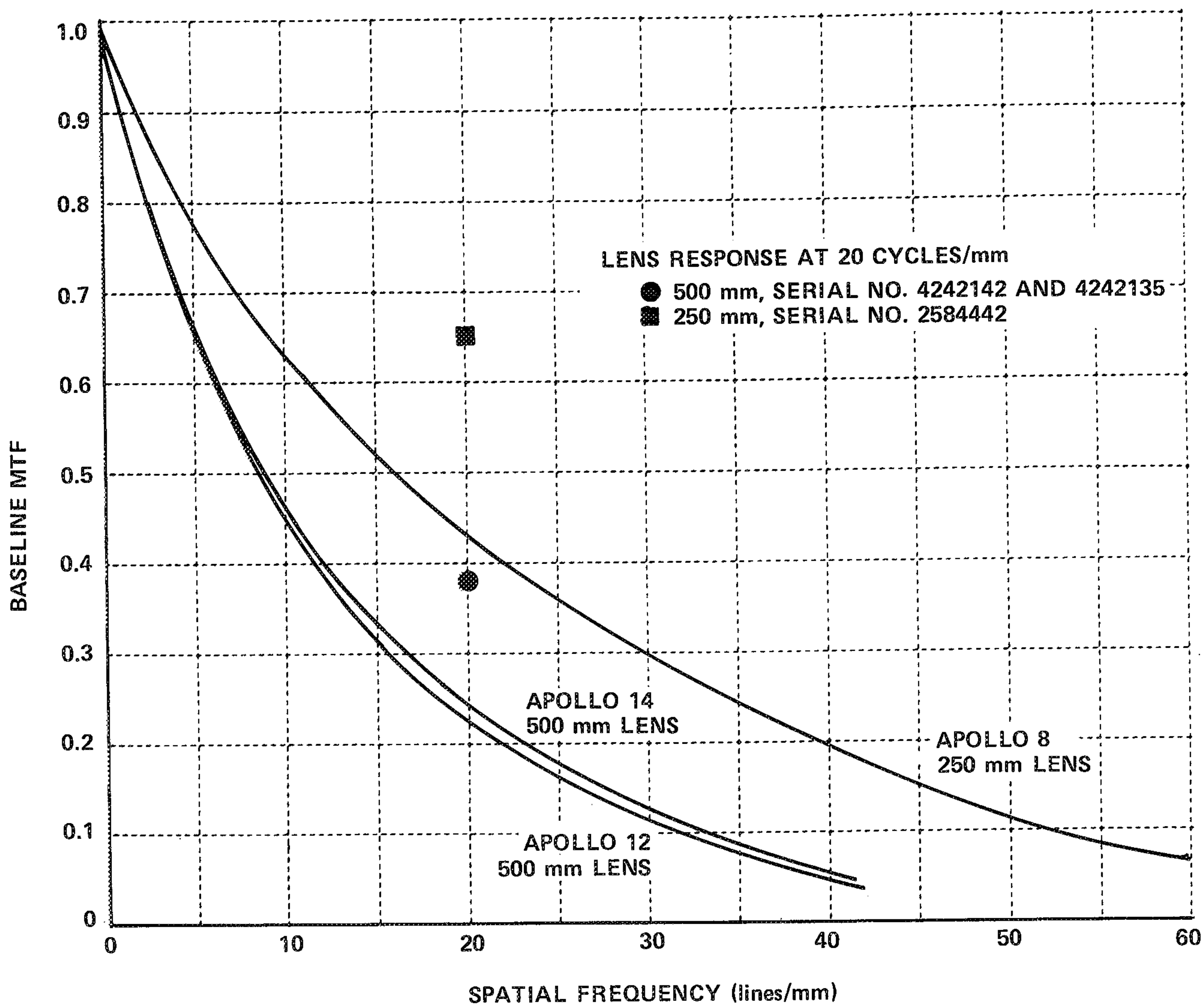

Figure 15 ESTIMATED BASELINE PERFORMANCE MODULATION TRANSFER FUNCTIONS

The exposure function is then differentiated and Fourier transformed to determine an estimate of the MTF for that frame. The individual estimates resulting from each of the edges selected in a given frame were combined to determine an average MTF and an associated 95% confidence band.

In selecting edges within an acceptable frame the only requirement is that the crater be small enough in size so that the penumbra length does not affect the measurement of the modulation transfer function.(1) By selecting craters smaller than 1mm in diameter on the film this requirement was fulfilled for Hasselblad photography with the 250mm or 500mm lenses. Table 6 indicates the amount of data collected for each of the missions.

Table 6

EDGE DATA COLLECTED AND PROCESSED FOR APOLLO 8, 12 AND 14

APOLLO MISSION NO.	FRAME	NO. OF EDGES
8	2300	12
	2301	15
	2302	15
	2303	15
	2304	15
	2307	15
12	7833	11
	7834	15
14	9520	1
	9521	2

In the case of the Apollo 8 photographs the frames analyzed were taken at low sun elevation angles and the major portion of the crater, about 90%, was in shadow. Therefore the shadow-to-sunlight edge interior to the crater and a second edge at the rim of the crater were separated by distances on the order of 1/10 of a millimeter or less. Consequently, the exposure function from the two edges may very well overlap and interfere somewhat with determination of the exposure function for the shadow-to-sunlight edge alone. Although this was not judged to be a serious limitation it does reduce the accuracy of the analysis techniques to some degree.

The modulation transfer function measured for each of the photographic frames were divided by the appropriate baseline MTF presented previously in Figure 15. The resulting residual MTF represents that attributed to the uncompensated motion smear in the photograph. The results for Apollo 8 are shown in Figures 16-21 along with the theoretical modulation transfer function expected if no compensation were achieved in the imagery (dashed curve).

As a result of studies we have made on the accuracy and precision of estimating modulation transfer function by using the modulus averaging technique employed in this study, we have found that it underestimates the modulation transfer function at the lower spatial frequencies and overestimates the modulation transfer function at the higher frequencies. These errors become worse as the noise fluctuations in the edge trace increase. Our earlier work[4] has also shown that the average modulation transfer function will not approach zero response as the theoretical MTF for linear motion smear indicates because of a positive bias introduced by the noise in the edge trace. In order to estimate the amount of compensation achieved, the theoretical modulation transfer function for linear motion smear,

$$\tau(\nu) = \sin(\pi \nu x_0) / \pi \nu x_0 \tag{9}$$

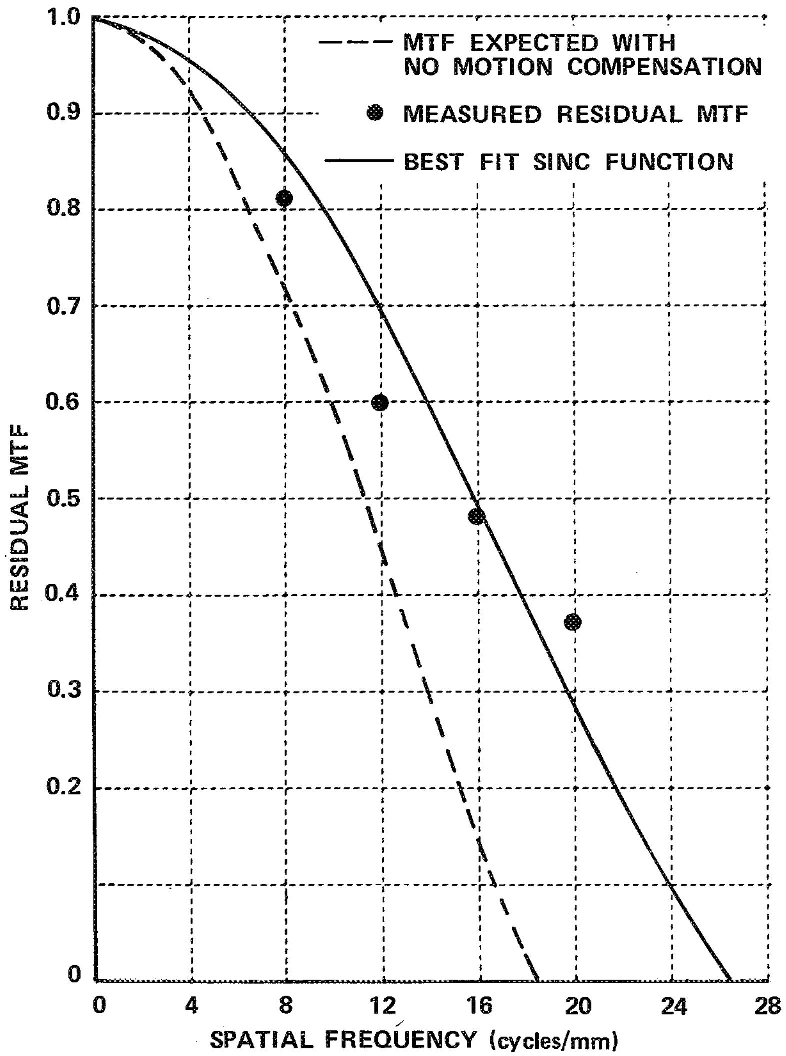

Figure 16 RESIDUAL MOTION SMEAR MTF – FRAME 2300, APOLLO 8

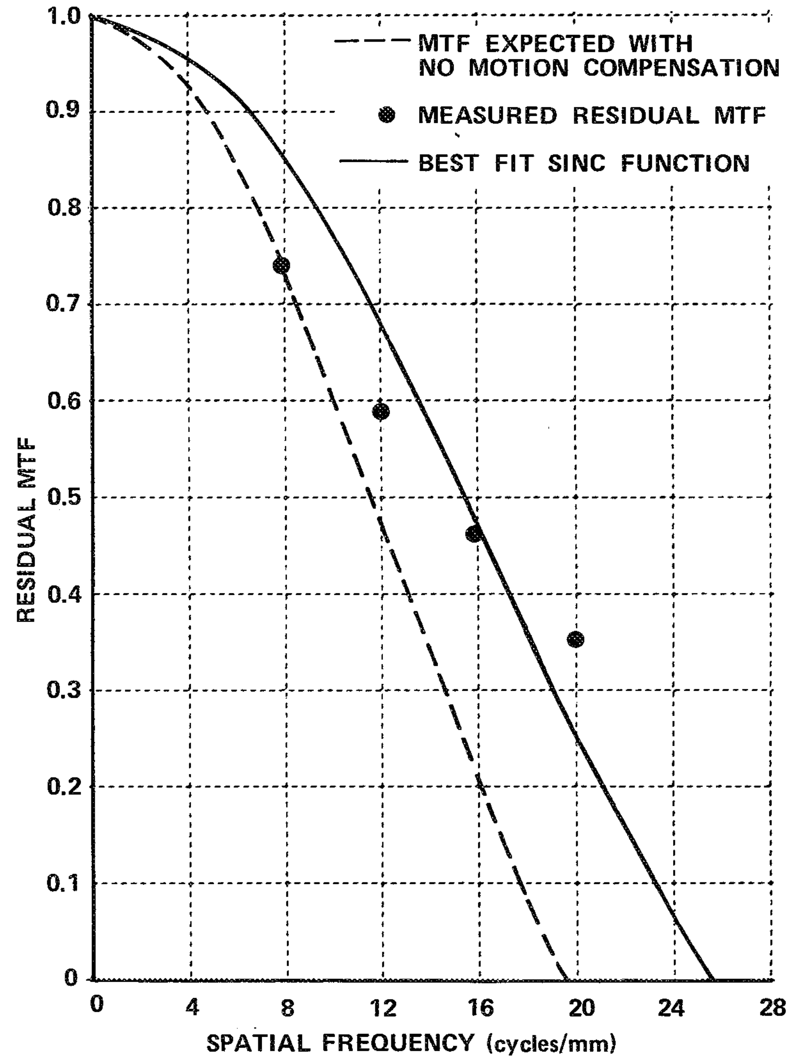

Figure 17 RESIDUAL MOTION SMEAR MTF – FRAME 2301, APOLLO 8

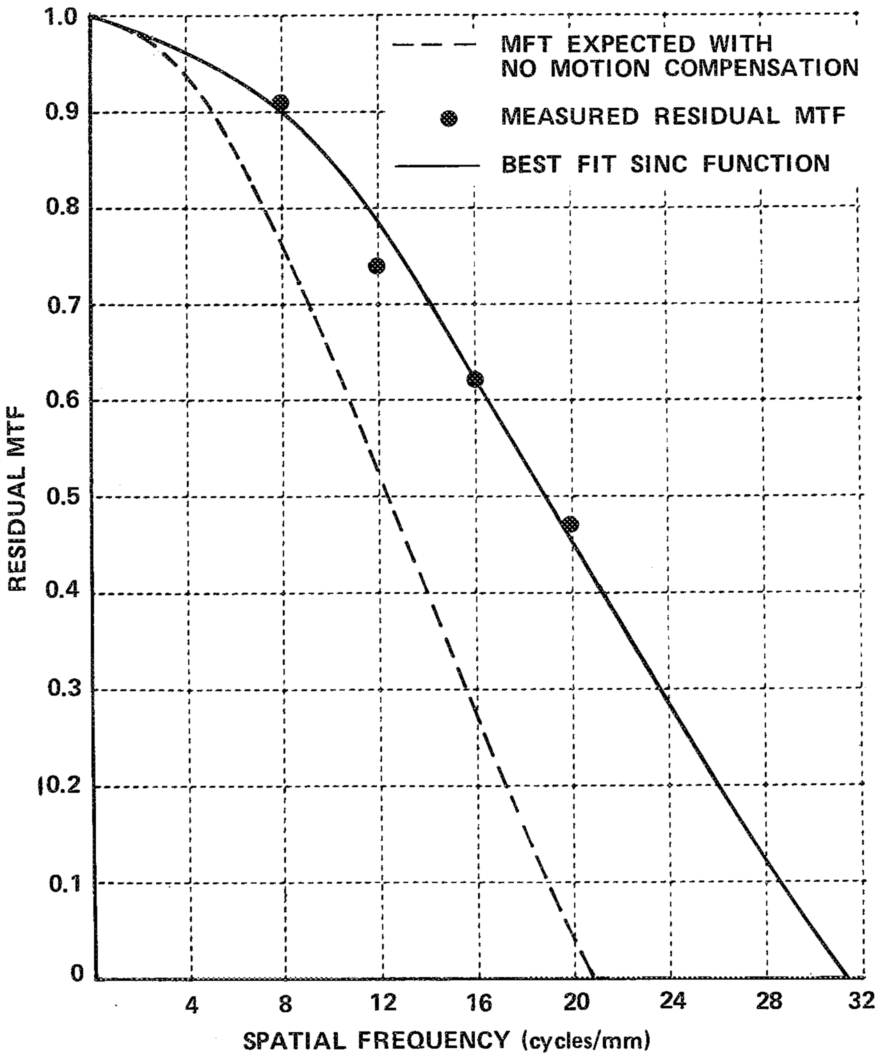

Figure 18 RESIDUAL MOTION SMEAR MTF – FRAME 2302, APOLLO 8

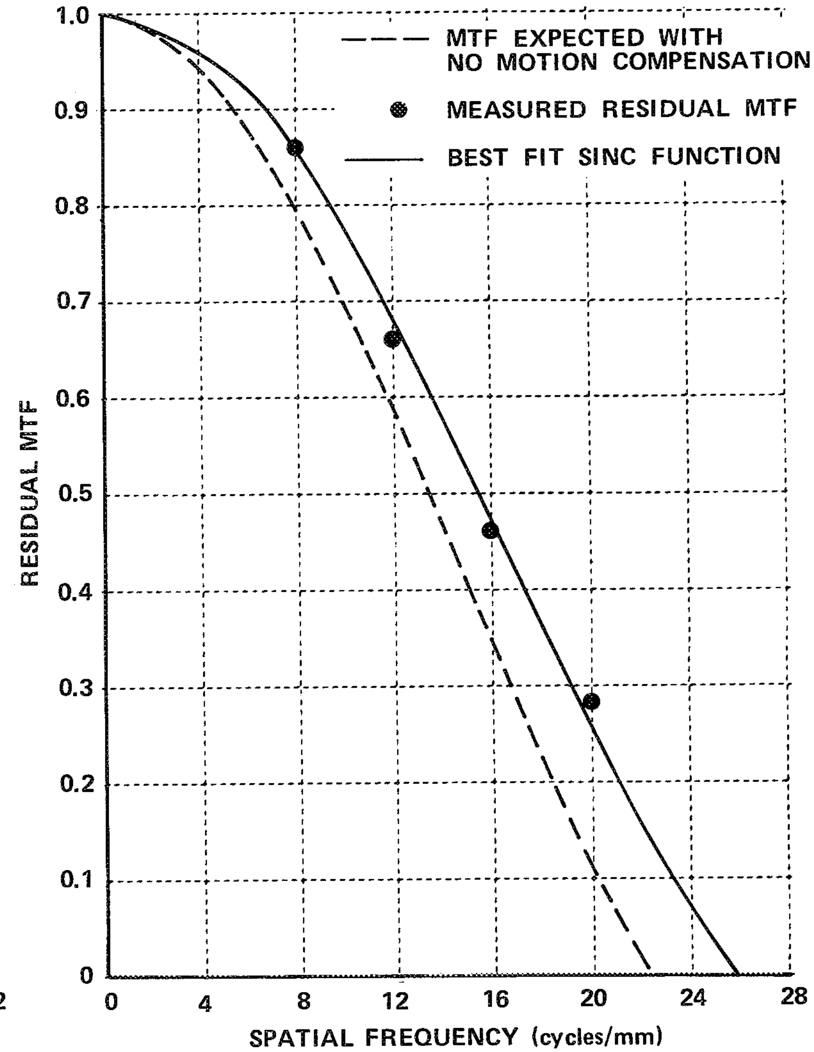

Figure 19 RESIDUAL MOTION SMEAR MTF – FRAME 2303, APOLLO 8

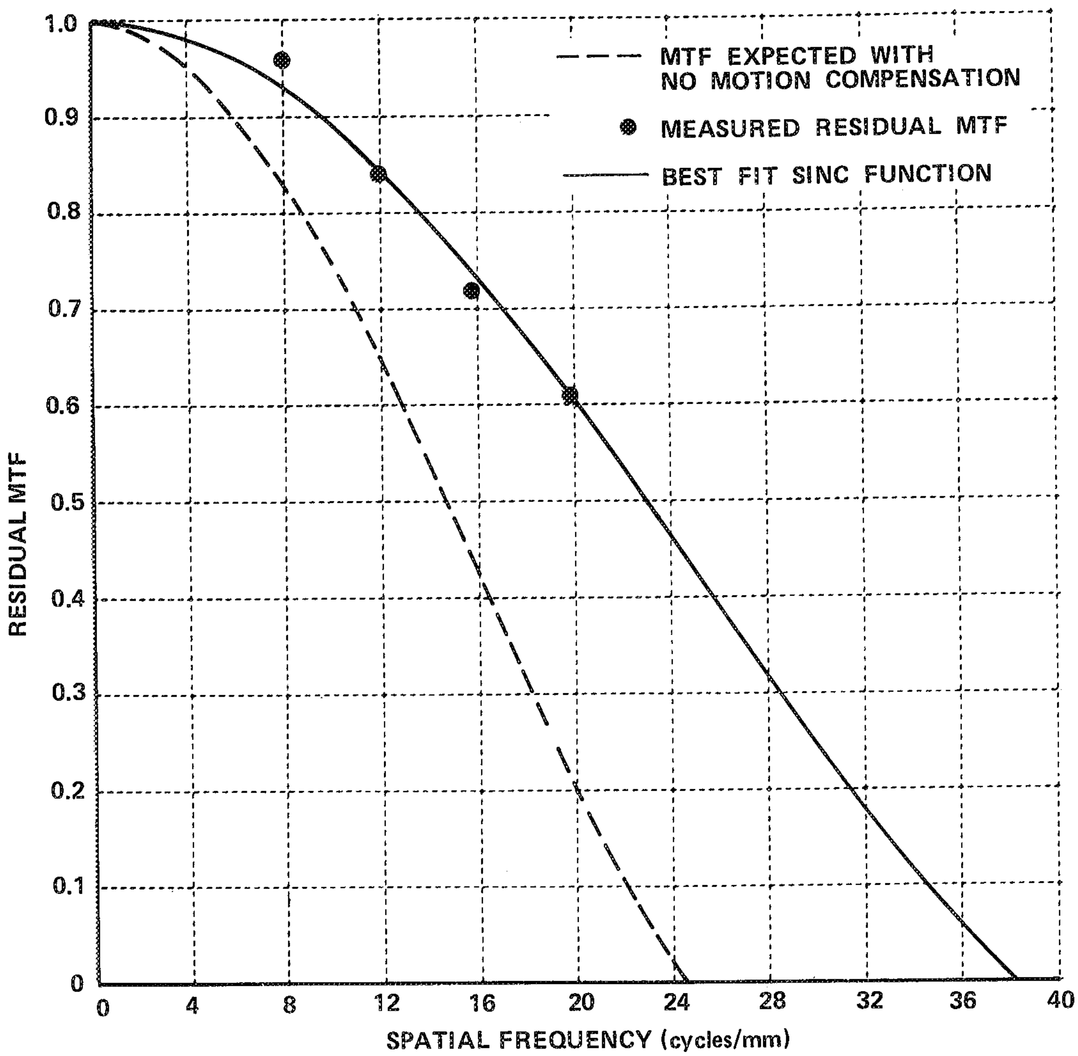

Figure 20 RESIDUAL MOTION SMEAR MTF - FRAME 2304, APOLLO 8

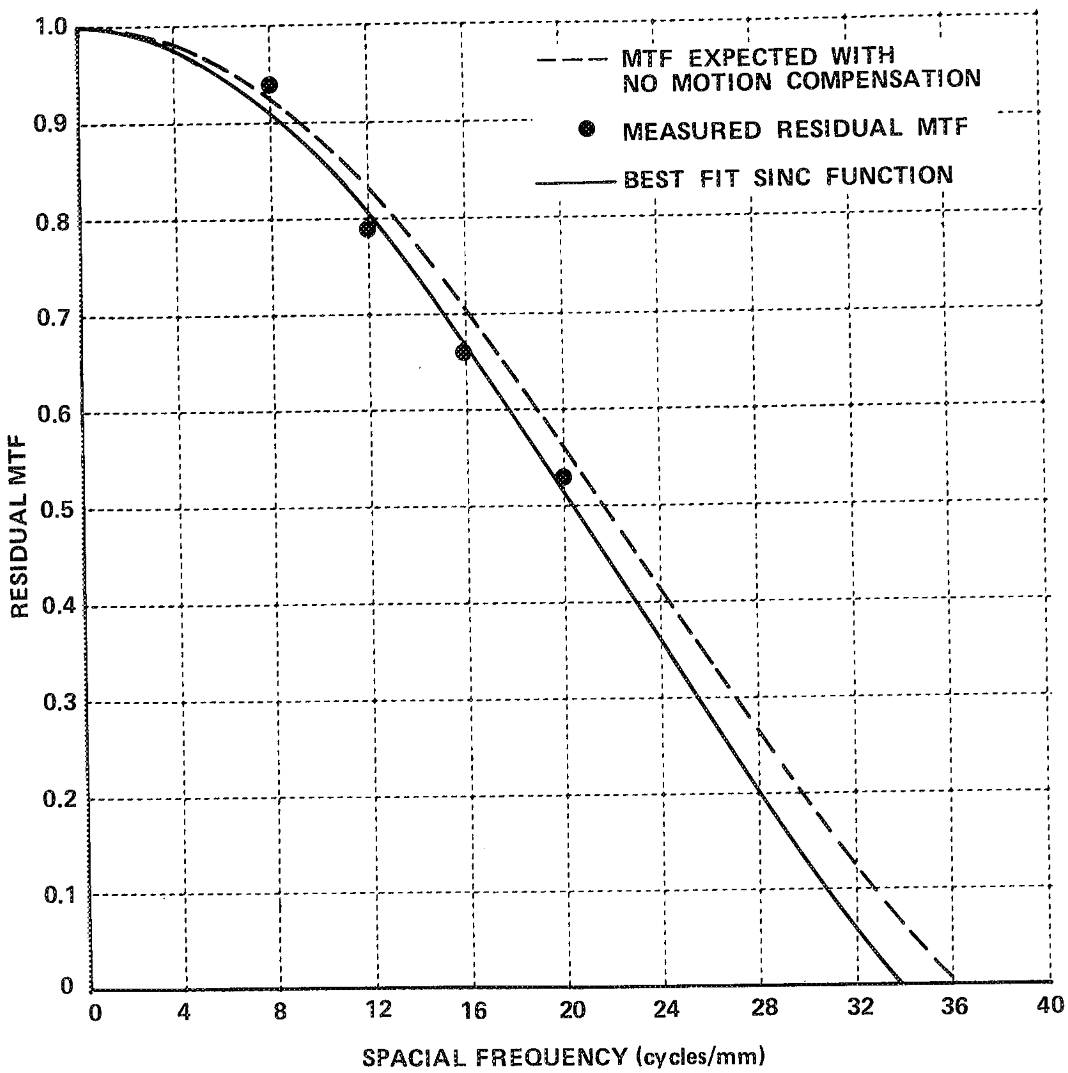

Figure 21 RESIDUAL MOTION SMEAR MTF - FRAME 2307, APOLLO 8

where χ_o is the amount of smear in the image, was fit to the measured residual modulation transfer function in the mid-frequency region, where the averaging technique is most accurate. The measured responses due to residual smear (solid dots in Figures 16-21) were fitted to the theoretical expression using non-linear estimation methods based upon the least-squares criterion. The resulting curves are shown as the solid line in the figures. The zero of the fitted curves were used to estimate magnitude of the residual smear at the film plane and compared to that expected without no motion compensation. The results are presented in Table 7. About 30% of the motion was compensated improving the ground resolution from 27 to better than 20 meters.

Table 7
MOTION COMPENSATION ACHIEVED
(APOLLO 8 PHOTOGRAPHY)

FRAME NO.	MOTION SMEAR (MICRONS ON FILM)		COMPENSATION ACHIEVED	SMEAR AT LUNAR SURFACE (METERS)
	WITHOUT IMC	RESIDUAL		
2300	54	38	31%	17
2301	51	39	24%	18
2302	48	32	34%	16
2303	45	39	14%	21
2304	41	26	36%	15
2307	28	30	NONE	26

In the case of the Apollo 12 analysis the achieved MTF fell below the baseline MTF by more than the degradation attributable to full uncompensated motion blur. It is quite likely that the measurement of the achieved MTF is inaccurate due to the high solar angle and the difficulty in identifying shadow-to-sunlight edges in the imagery. No attempt was made to edit the edge data or find other suitable targets in the selected frames.

As shown earlier, a bright ray was located on Frames 9520 and 9521 of the Apollo 14 imagery. A limited number of microdensitometer scans were made across the edge of the ray in an attempt to evaluate the residual smear in the imagery. Figure 22 shows the results obtained from

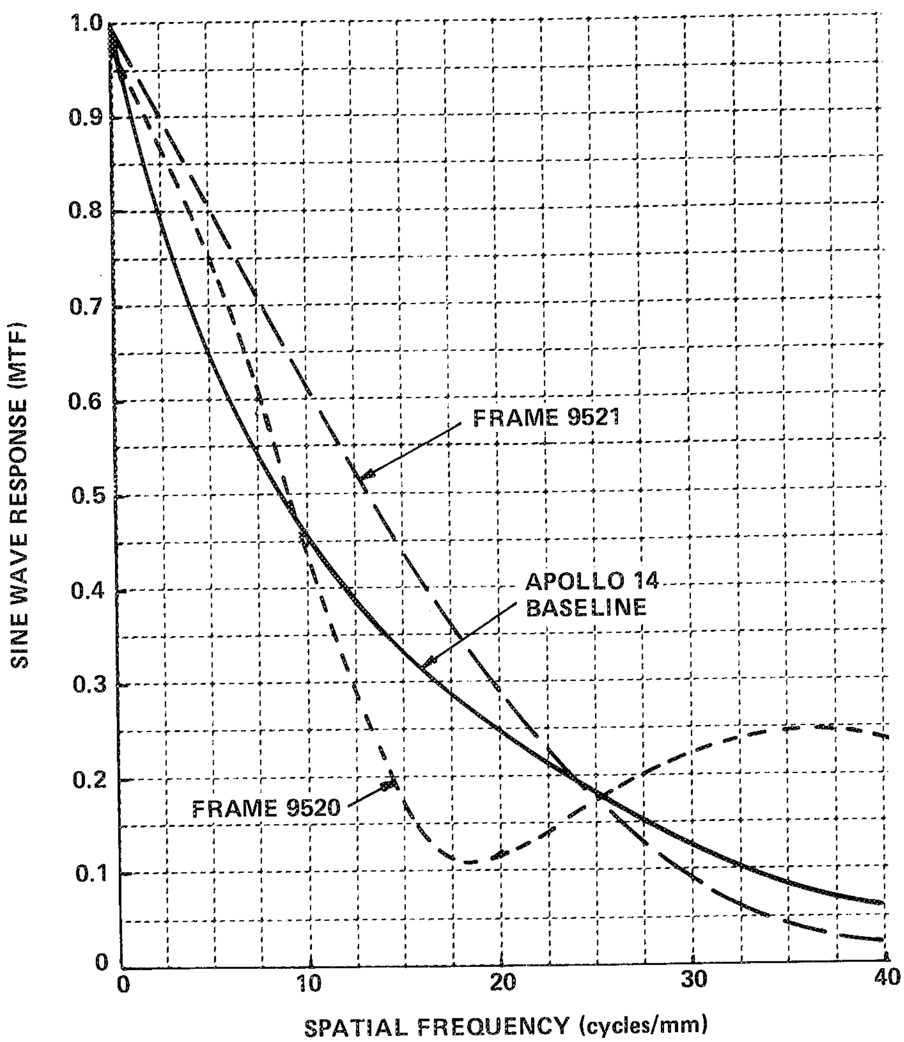

Figure 22 ACHIEVED MTF COMPARED TO ESTIMATED BASELINE FOR APOLLO 14 PHOTOGRAPHY

a single edge trace on each frame. Considering the limited amount of data available and the fact that the Apollo 14 500mm lens could have an MTF different from the average of the lens bench tests presented earlier in Figure 5 the results indicate that it is likely that a considerable percentage of the motion of the Command Module was compensated.

4. ASSESSMENT OF DETAIL LOSS IN REPRODUCTION

Usually none of the users of Apollo orbital photography work directly with the flight film. Instead they receive a second or fourth generation copy. As a result, some of the tasks in this study were concerned with assessing the detail loss, if any, that occurs as a result of reproduction. Two sources of detail loss were evaluated; loss in resolution or fine detail as measured by the MTF and the loss in contrast as measured by the sensitometric calibration. Fortunately, the calibration step tablets exposed onto and processed with the original flight film were also copied during the reproduction process. Therefore, we can relate the sensitometric calibration curve for each copy to relative lunar surface radiance.

4.1 Resolution Loss in Reproduction. - An evaluation of the loss in resolution or fine detail due to reproduction was made for the Apollo 8, 12 and 15 missions. On Apollo 12 and subsequent missions a second set of tri-bar resolution charts was available. These charts were included in the step tablets exposed onto the leader of the flight film. Since these charts did not pass through the 80mm or any other lens, whereas the NBS resolution chart did, the MTFs determined from these two data sources should differ by the combined effect of the MTF of the 80mm lens and any additional operational degradations (i.e. film buckle, defocus, etc.). The MTF obtained from the charts in the sensitometric data represent the combined degradation of the flight film, processing and reproduction steps.

Analysis of the NBS resolution chart on the flight film and a 2P copy of Apollo 8 produced the results shown in Figure 23. They show reasonable agreement and consequently it is concluded that the Apollo 8 copies faithfully reproduce the detail content contained in the original flight film.

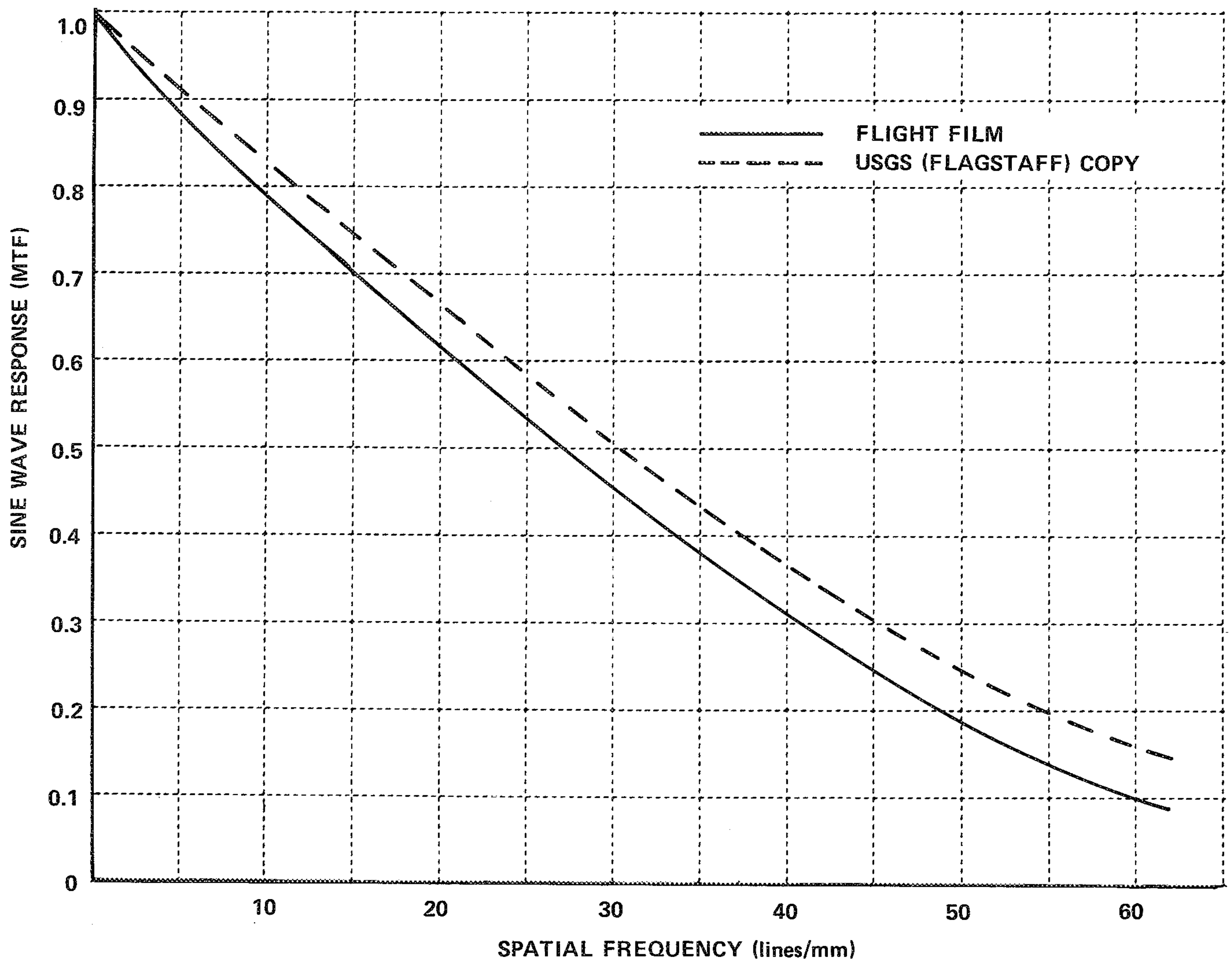

Figure 23 MEASURED SINE WAVE RESPONSE – NBS RESOLUTION CHART – APOLLO 8, MAGAZINE E

For the Apollo 12 mission a slightly expanded analysis was performed; the flight film and two different 2P copies were evaluated. One of the 2P copies was made available by the Mapping Sciences Laboratory (MSL) at the NASA Manned Spacecraft Center and the other by the USGS Center for Astrogeology at Flagstaff, Arizona. The tri-bar resolution chart included in the sensitometric data was evaluated on both 2P copies as well as the original flight film. The methods described in Section 2.2 were used to obtain an estimate of the combined film-processing-reproduction MTF and the results in Figure 24 obtained. The agreement between the copies and the flight film is evident indicating that there is little loss in resolution during reproduction.

The NBS Resolution Charts were also evaluated on the flight film and both copies. These were reduced to obtain the achieved MTFs presented in Figure 25. During the return flight of Apollo 12 several photographs were taken through the 80mm lens of the lunar disk. Because of the characteristics of the lunar photometric function the disk is uniform and its edges form suitable targets for evaluating the MTF. Consequently the edge of the lunar disk was scanned in frames 7887 and 7888 on one of the 2P copies. The resulting microdensitometer traces were processed using the methods described in Section 2.3 to obtain a second estimation of the achieved MTF. As can be seen from the Figure both results are in agreement.

If we compare the baseline MTF of the Apollo 8 80mm lens presented in Figure 23 to the corresponding baseline MTF for Apollo 12 in Figure 25 we see that Apollo 12 80mm photography suffered a considerable fine detail degradation compared to the Apollo 8 80mm photography.

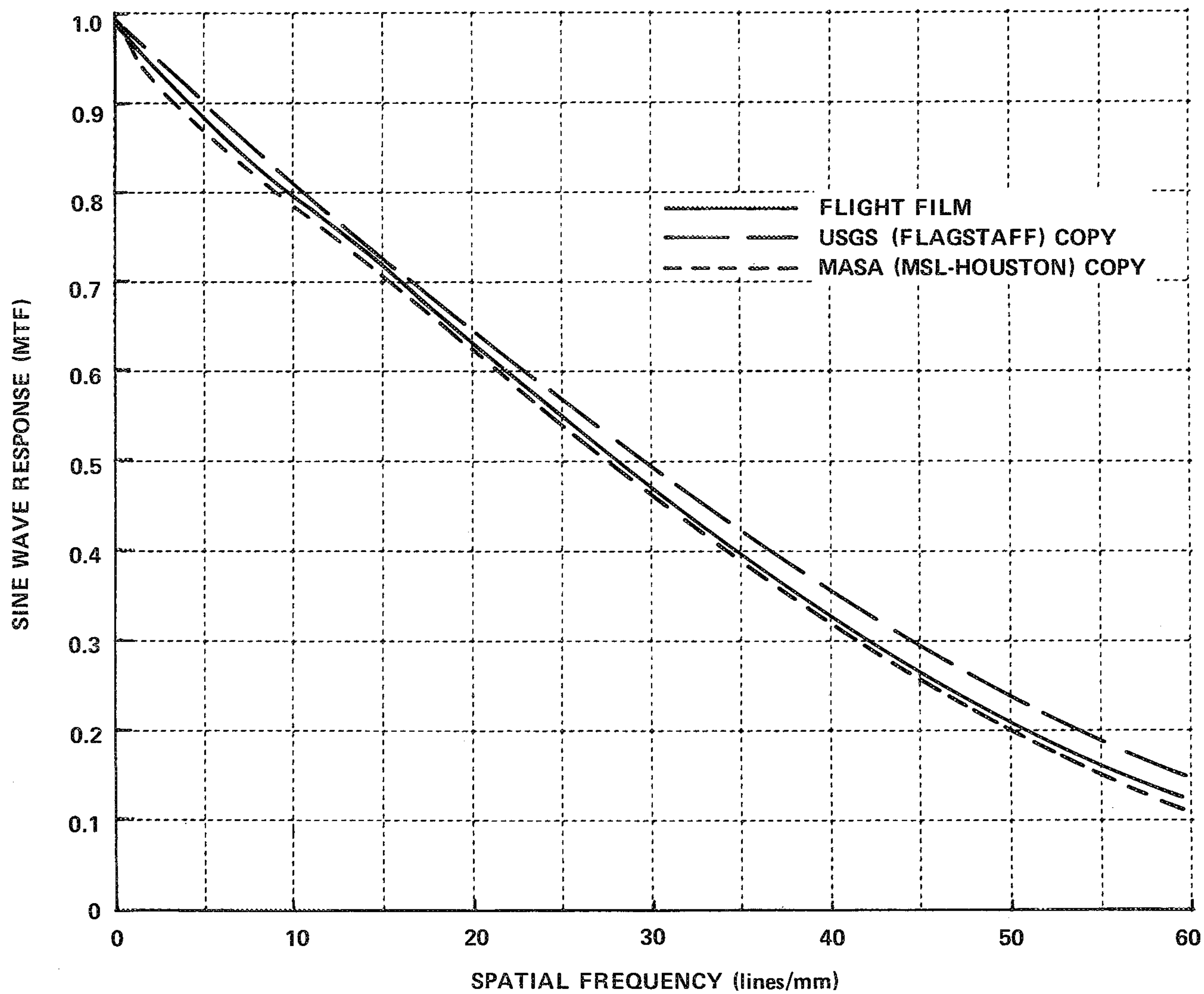

Figure 24 MEASURED SINE WAVE RESPONSE – RESOLUTION CHARTS IN SENSITOMETRIC DATA APOLLO 12, MAGAZINE U

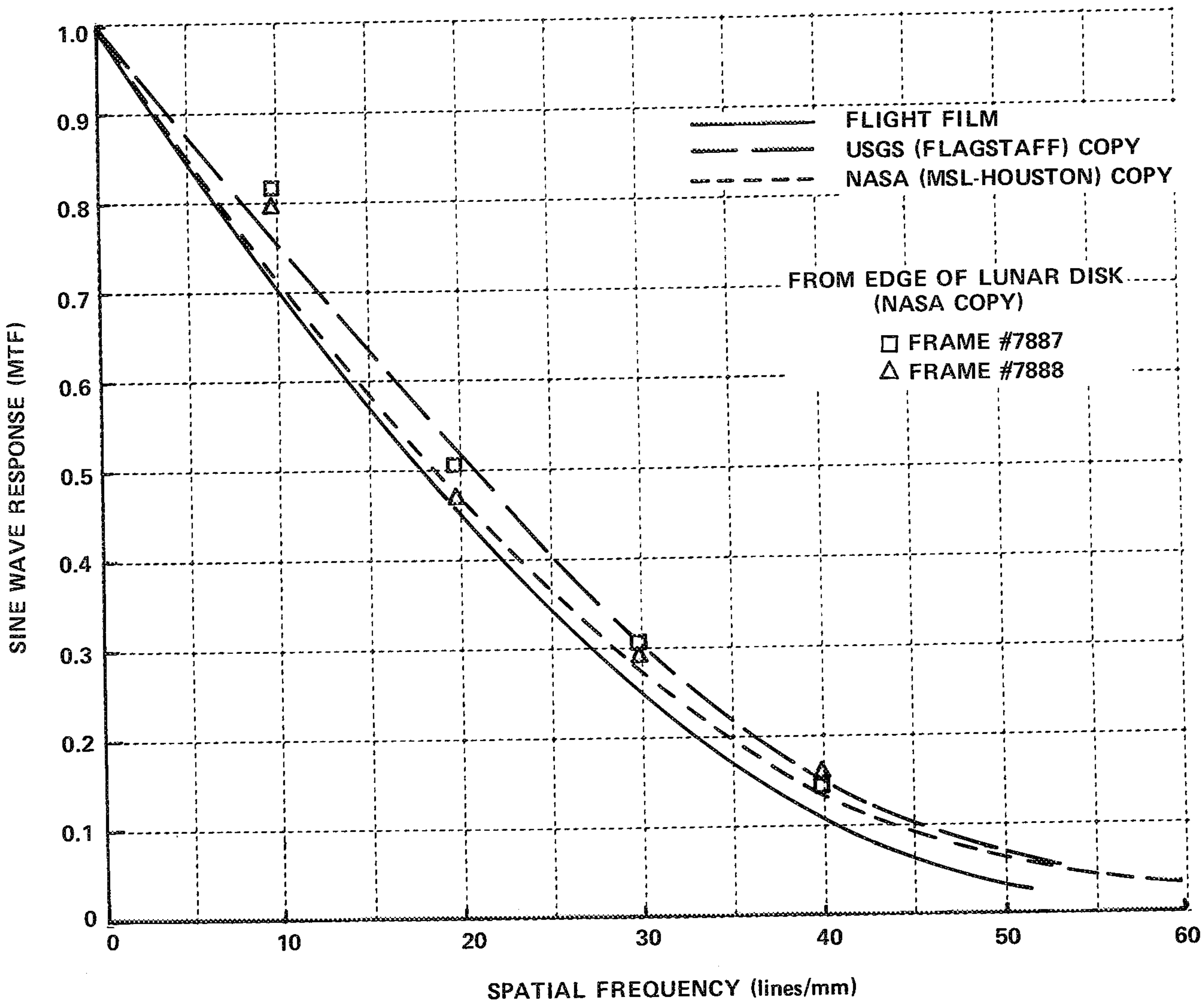

Figure 25 MEASURED SINE WAVE RESPONSE – NBS RESOLUTION CHART – APOLLO 12, MAGAZINE U

Because there are no resolution charts in the sensitometric data in the Apollo 8 imagery, no estimate of its 80mm lens performance can be made. It is unlikely however that the measured performance would be equivalent to the bench test shown previously in Figure 5. Even if the operational lens performance and the bench test performance were equivalent in the case of Apollo 8, this would only account for half of the observed difference of the detail content between the two missions. Since this is unlikely it is concluded that the major portion of the difference between the detail content is due to the change in the type of film between the two missions. In the Apollo 8 mission flight film consisted of Eastman Kodak Type 3400 whereas in the Apollo 12 mission the film employed was SO-164. Both films have identical emulsion characteristics, however, the special order film (SO-164) lacks an anti-hilation backing. Without this backing light can be scattered into the emulsion from the back side of the film and thus decreasing the detail rendition capability of the film.

An analysis of Apollo 15 metric and panoramic imagery was also undertaken to determine the loss of information, if any, in higher generation reproductions. Visual inspection of enlargements made by some of the users had indicated a softening of some detail particularly within shadowed and bright surface areas. The objective was to determine whether this loss occurred in the reproduction processes and suggest potential methods for correction that could be applied to Apollo 16 imagery.

Measurements were made in two categories of image quality; fine detail rendition and contrast reproduction. In this section we discuss the results of the assessment of the loss of fine detail or "resolution". Two frames were selected from the metric camera photography and two frames from the panoramic camera photography. In both cases the frames were selected so that the sun angle produced a suitable shadow-to-sunlight edge interior to the crater; 5^o -15^o sun elevation. In selecting the panoramic imagery additional consideration was given to the motion smear compensation because of the irradic performance of the V/H sensor during the Apollo 15 mission. Frames were selected where the V/H command was locked on to the nominal rate thus providing approximate compensation of the motion smear and improved resolution on the original film for that frame.

Metric camera photographs, Frames 81 and 2219, and Panoramic camera photographs, Frames 350 and 8850, were selected for analysis. The modulation transfer function was evaluated for the original flight film, a direct duplication negative (2N), a master positive (2P) and a fourth generation positive (4P). Shadow-to-sunlit edges interior to small craters (in the range of 50 to 100 microns in diameter on the film) were scanned using a microdensitometer. The four frames of original flight film and the master positive of Frame 8850 were scanned using the Mann Microanalyzer available at the Manned Spacecraft Center. All of the other imagery was scanned using the Mann Microdensitometer available at our Laboratory; both instruments are similar.

In order to minimize the degrading effects of the measuring instrument upon the edge trace, as small as possible scanning aperture was employed; a five micron diameter spot in the MSC instrument and a 2x2 micron square aperture in our instrument. In the latter case the finite resolution of the microscope objective broadened the scanning aperture so that it also is reasonably represented by a 5 micron diameter circle.

In selecting the craters for analysis an upper bound was placed upon the crater diameter by requiring that the penumbra effect, which reduces the edge sharpness, be about 1/10 the resolution anticipated from the camera system. This problem was previously considered in the evaluation of Lunar Orbiter imagery(6) and the results reported were employed to establish the acceptable crater size for analysis.

Table 8 shows the number of edges scanned for each of the frames of photography analyzed. Each of the edge scans or edge traces was processed using the techniques described previously in Section 2.3. The results we

Table 8
EDGE DATA COLLECTED AND PROCESSED FOR
FOR APOLLO 15 PHOTOGRAPHY

FRAME \ TYPE	FLIGHT	DIRECT NEGATIVE	MASTER POSITIVE	4th GEN. POSITIVE
81	12	20	7	14
2219	14	11	16	13
350	13	25	13	14
8850	15	17	9	12

obtained in the analysis of the four frames of original flight film and the copies are shown in Figures 26 through 29. No corrections were employed to remove the loss in modulation introduced by the instrument (scanning) aperture or penumbra effect. We note that except for the 2N copy of Frame 2219 all of the metric camera imagery (Figures 26 and 27) show reasonable agreement between the measured MTF values, i.e. there is no statistically significant difference. In both cases the 4P copy indicates a possible small enhancement up to 50 cycles/mm. Comparison of the results for the panoramic imagery show agreement except for the 2N copy which has a possible loss in fine detail content. Comparison between the two frames, particularly for the flight film, however, indicate that Frame 250 has a higher response at all frequencies compared to Frame 8850. Part of this difference can be explained

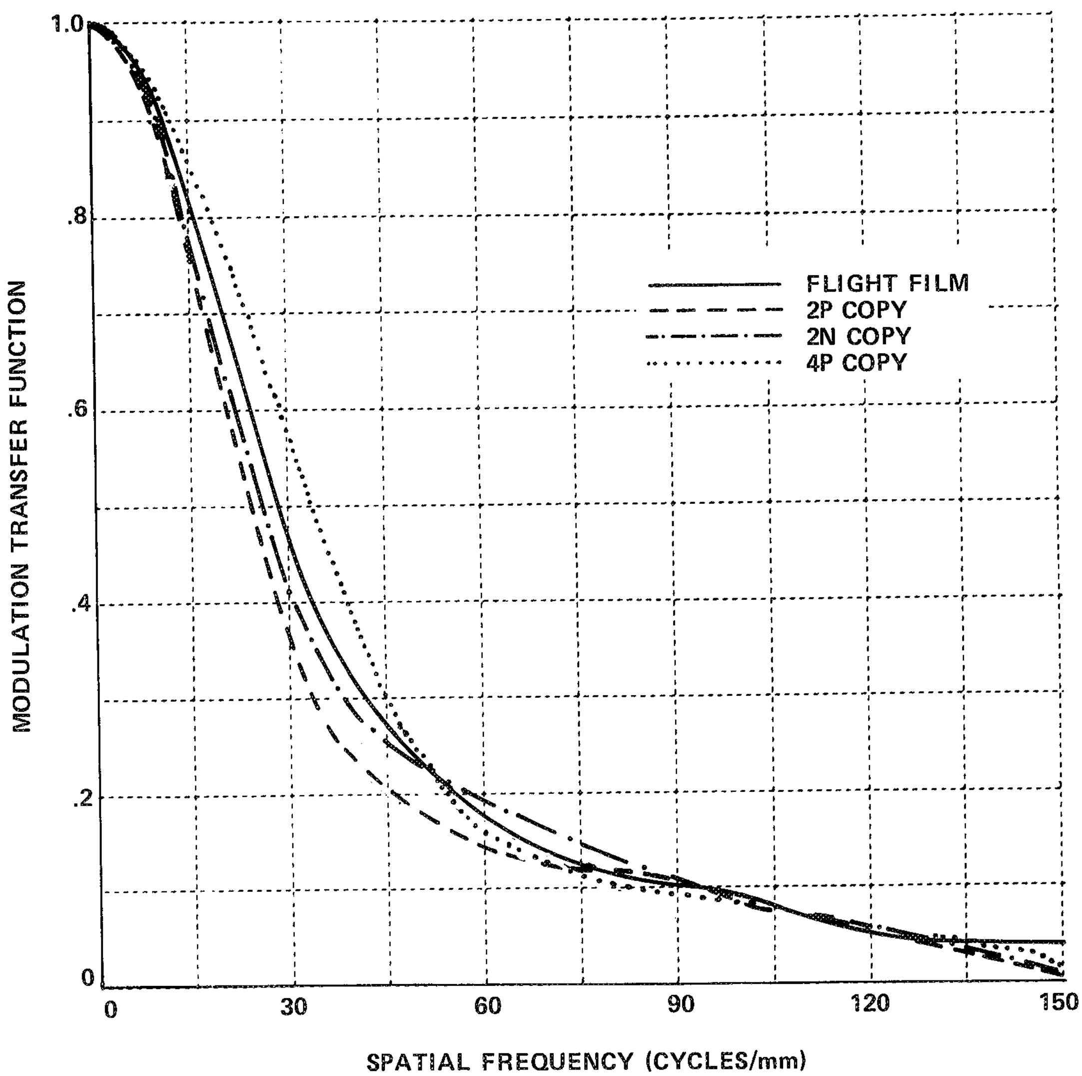

Figure 26 METRIC FRAME 81 FLIGHT FILM MTF

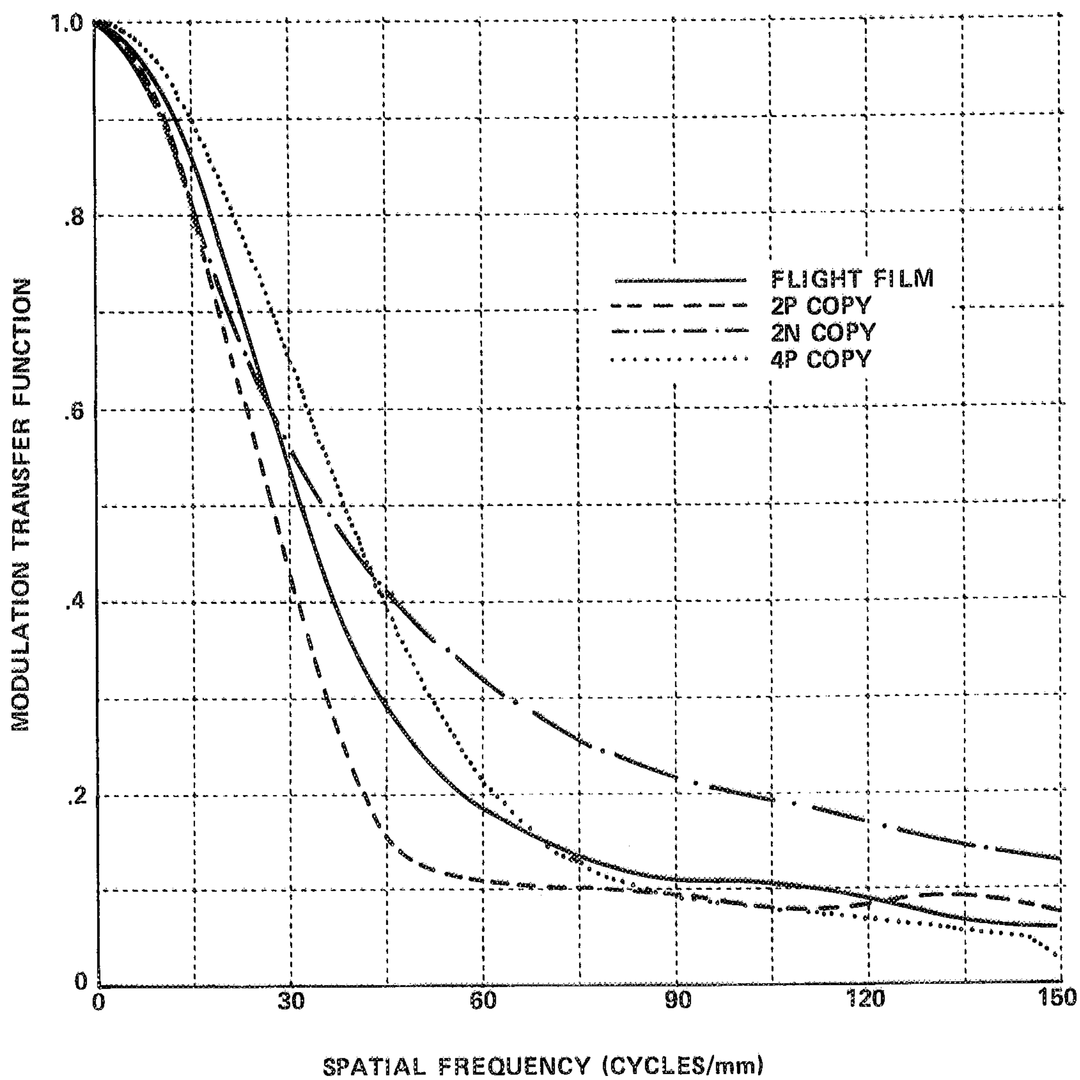

Figure 27 METRIC FRAME 2219 FLIGHT FILM MTF

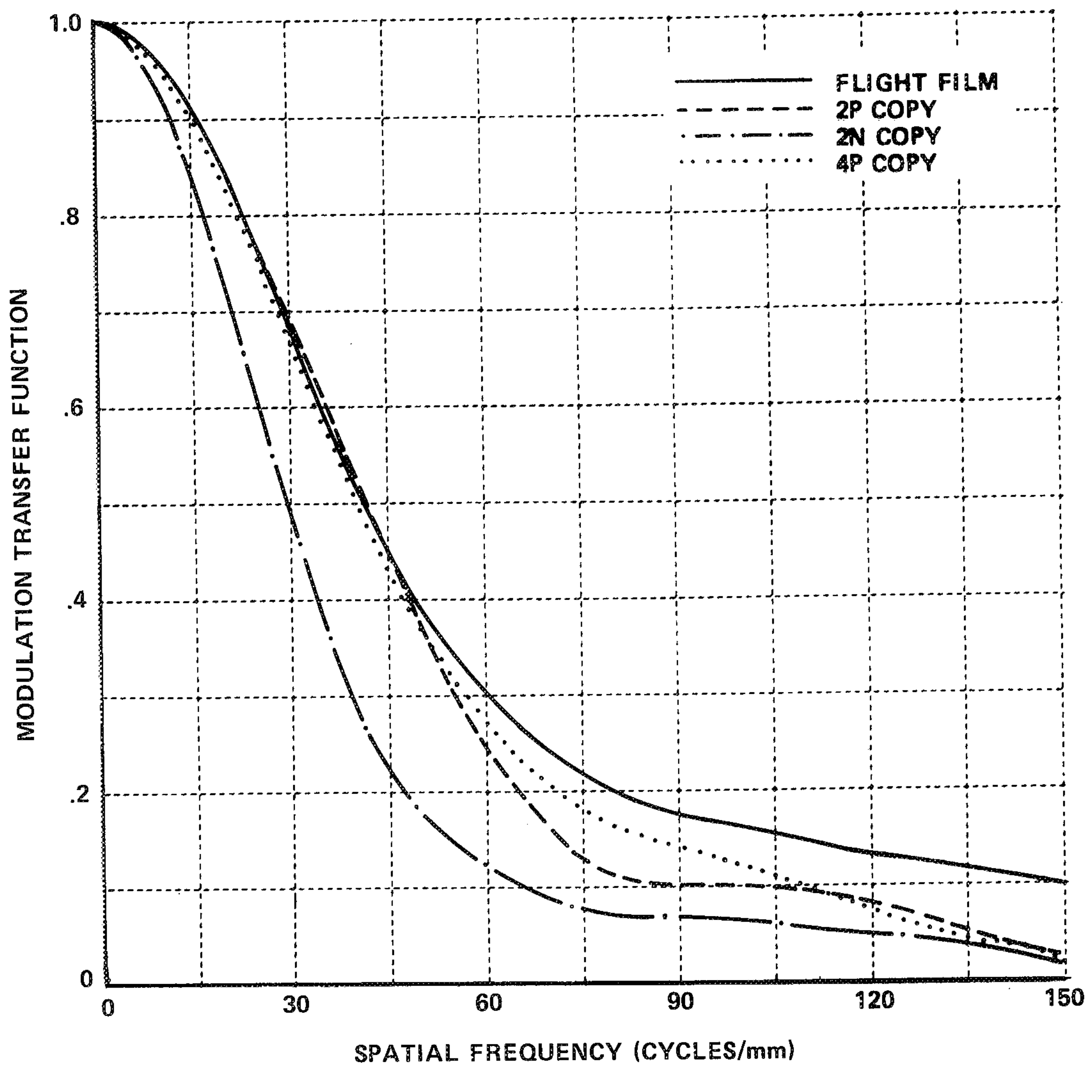

Figure 28 PAN FRAME 350 FLIGHT FILM MTF

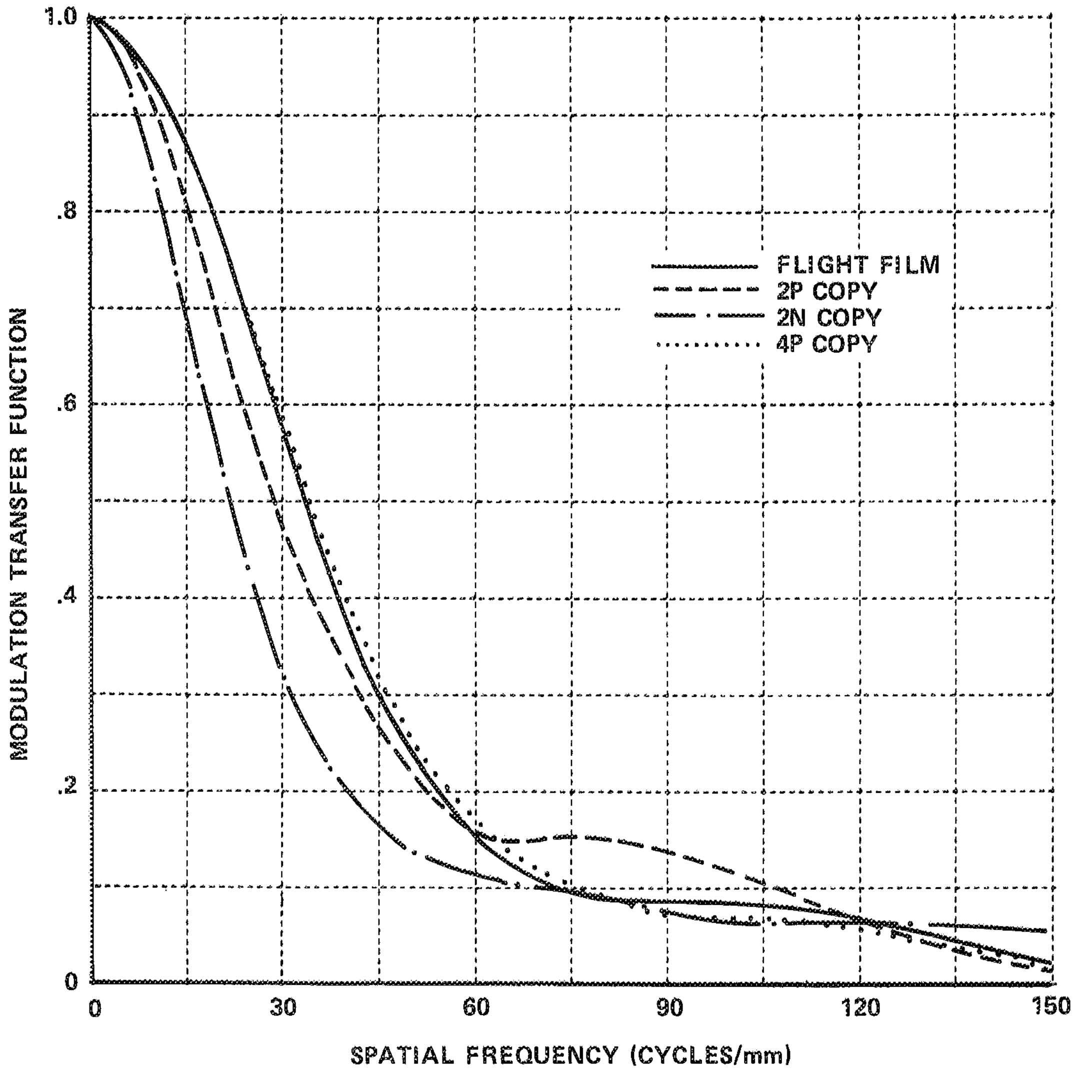

Figure 29 PAN FRAME 8850 FLIGHT FILM MTF

by the fact that the nominal V/H command rate at which both frames were taken compensates more fully for the actual V/H in the case of Frame 350. Several sources of auxilliary data were used to compute the residual V/H error for both of these frames. Telemetry data records were employed to compute the exposure time. These records contain the time interval when the capping shutter is open which corresponds to the time required to expose the total 45 inch long panoramic frame. From these data we computed the velocity of the exposing slit. The telemetry data also contains the width of this slit permitting the exposure time to be calculated. The results of these calculations yield a 0.013 second exposure time for Frame 350 and a 0.025 second exposure time for Frame 8850. The residual smear was calculated using the difference between V/H command contained in the telemetry data and the calculated V/H rate using the scaling presented previously in Eqs. (3a) and (3b). Frame 350 is oblique having a 12.4° tilt angle. The results of this calculation yield a residual smear of 6 microns at the film plane for Frame 350 and 30 microns for Frame 8850. Clearly the residual smear limits the resolution of Frame 8850 to about 33 cycles/mm while it will only have a slight effect in the case of Frame 350 thereby explaining the differences observed in Figures 28 and 29.

From the results presented in this section it is concluded that the loss of fine detail during the copying processes is not a major contributor to the apparent loss in detail observed by the users for the Apollo 15 imagery.

4.2 <u>Assessment of the Contrast Loss in Reproduction.</u> - In order to be able to determine the modulation transfer function using edge analysis the density trace across the edge must be converted to relative exposure. Consequently, the sensitometric data was obtained by scanning the step tablets on the original flight film and those reproduced in subsequent copies using the microdensitometer. The Huter-Driffield response curves obtained are shown in Figures 30 and 31 for the metric and panoramic cameras respectively.

The density difference across an object in an image can be altered by changing this response curve. In particular, a reduction in the density difference can be introduced by the toe and shoulder of the response curve if care is not taken to insure that the useful density range of the original image is copied well within the linear portion of the subsequent response curve for the copying process. We employed the sensitometric data we measured to evaluate the contrast reproduction of targets between the original flight film and higher generation copies. To do this we computed the density difference between adjacent steps of the step tablet. Adjacent steps correspond to an image on the original flight film with a ratio of the maximum exposure to minimum exposure of 1.4:1. The contrast of the original target on the lunar surface, of course, has been reduced by the combined performance of the flight lens and film to obtain an image with this contrast. If we assume that the target size is such that it lies in the neighborhood of the 0.25 response point of the flight film modulation transfer function, then the density differences between the adjacent steps correspond to a lunar surface target having an inherent contrast of 5:1. This contrast is probably too low for a crater with a shadow and too high for structure produced by albedo differences. However, it represents a reasonable compromise for the evaluation of the effect of the sensitometry upon the contrast reproduction in the flight film compared to the higher generation copies.

The results we obtained are presented in Figures 32 and 33. Figure 33 showing the contrast reproduction in the case of the panoramic camera clearly indicates that the density difference across the target in the copies as well as the flight film will be approximately the same except for bright lunar surface areas where the flight film shows an obviously higher image

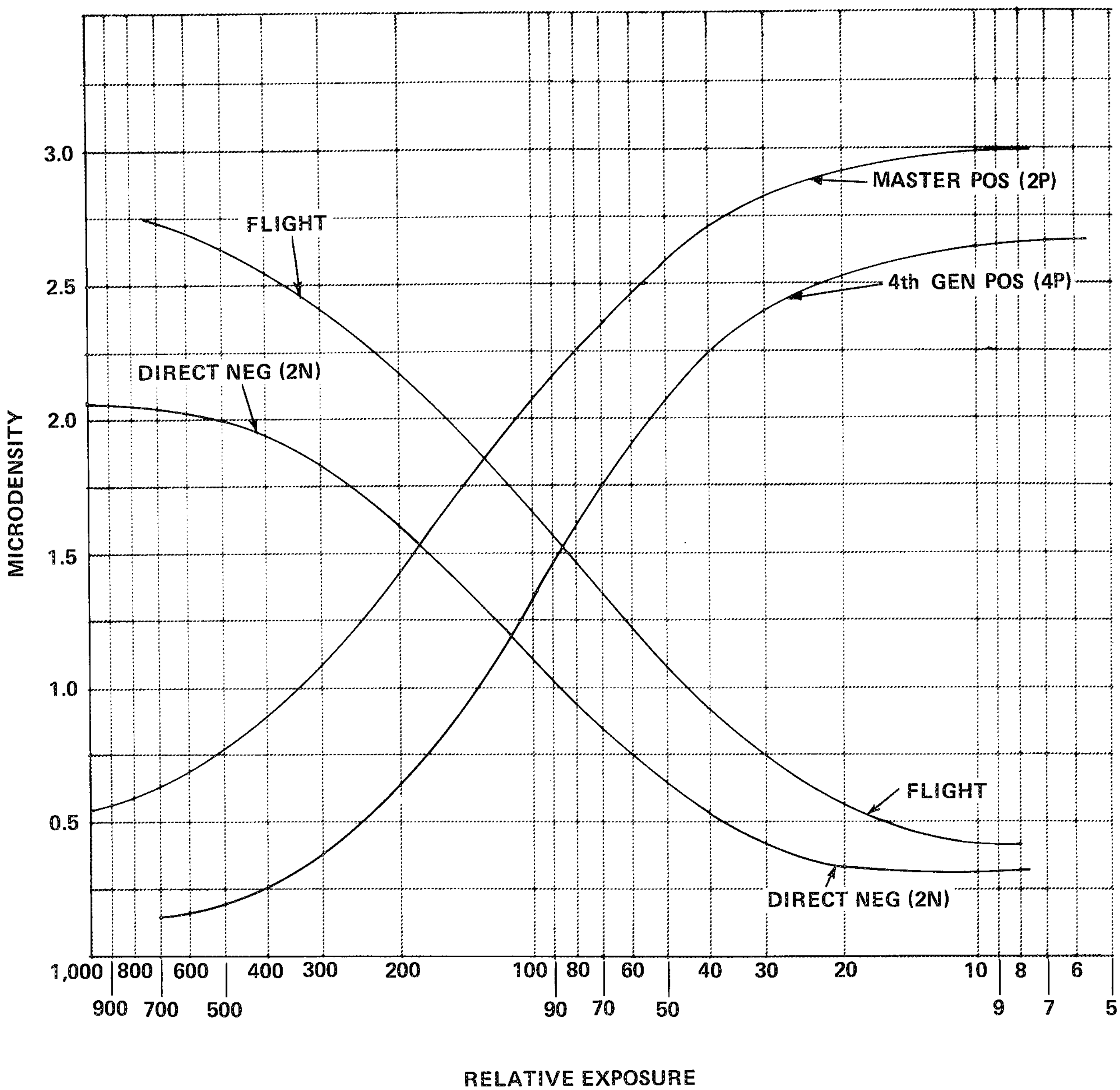

Figure 30 SENSITOMETRIC CALIBRATION – APOLLO 15 – METRIC

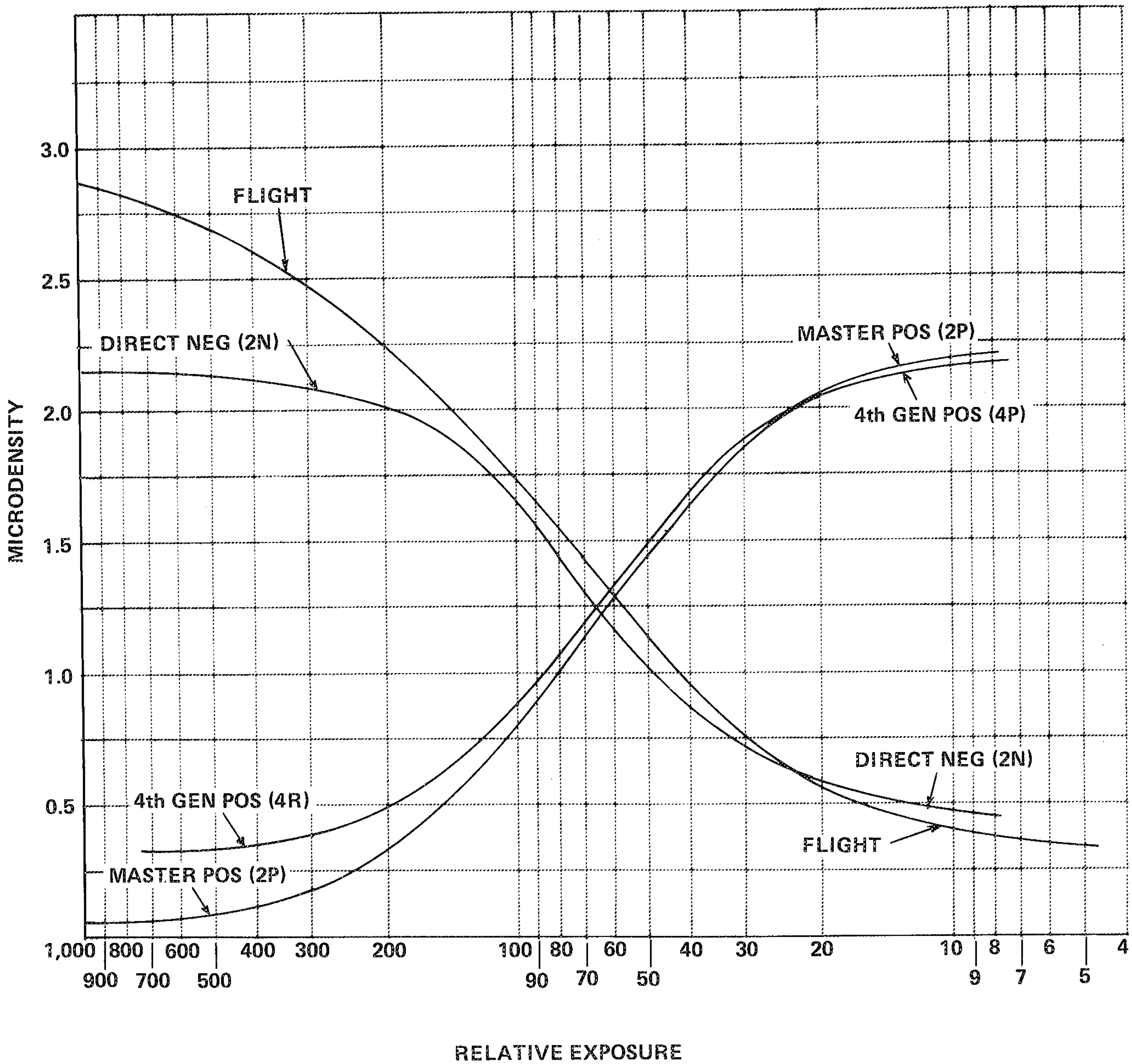

Figure 31 SENSITOMETRIC CALIBRATION – APOLLO 15 PAN

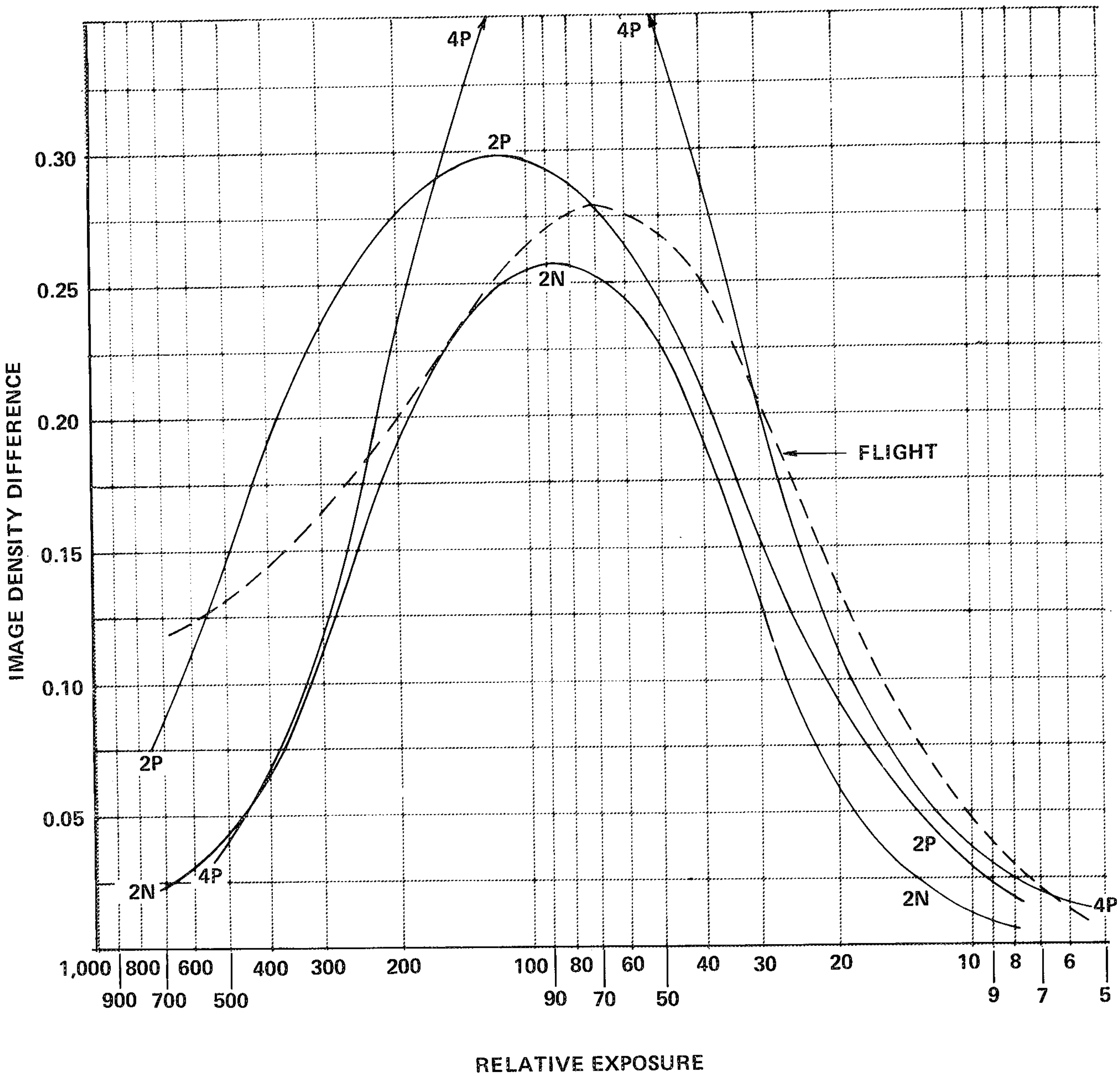

Figure 32 METRIC CAMERA CONTRAST REPRODUCTION

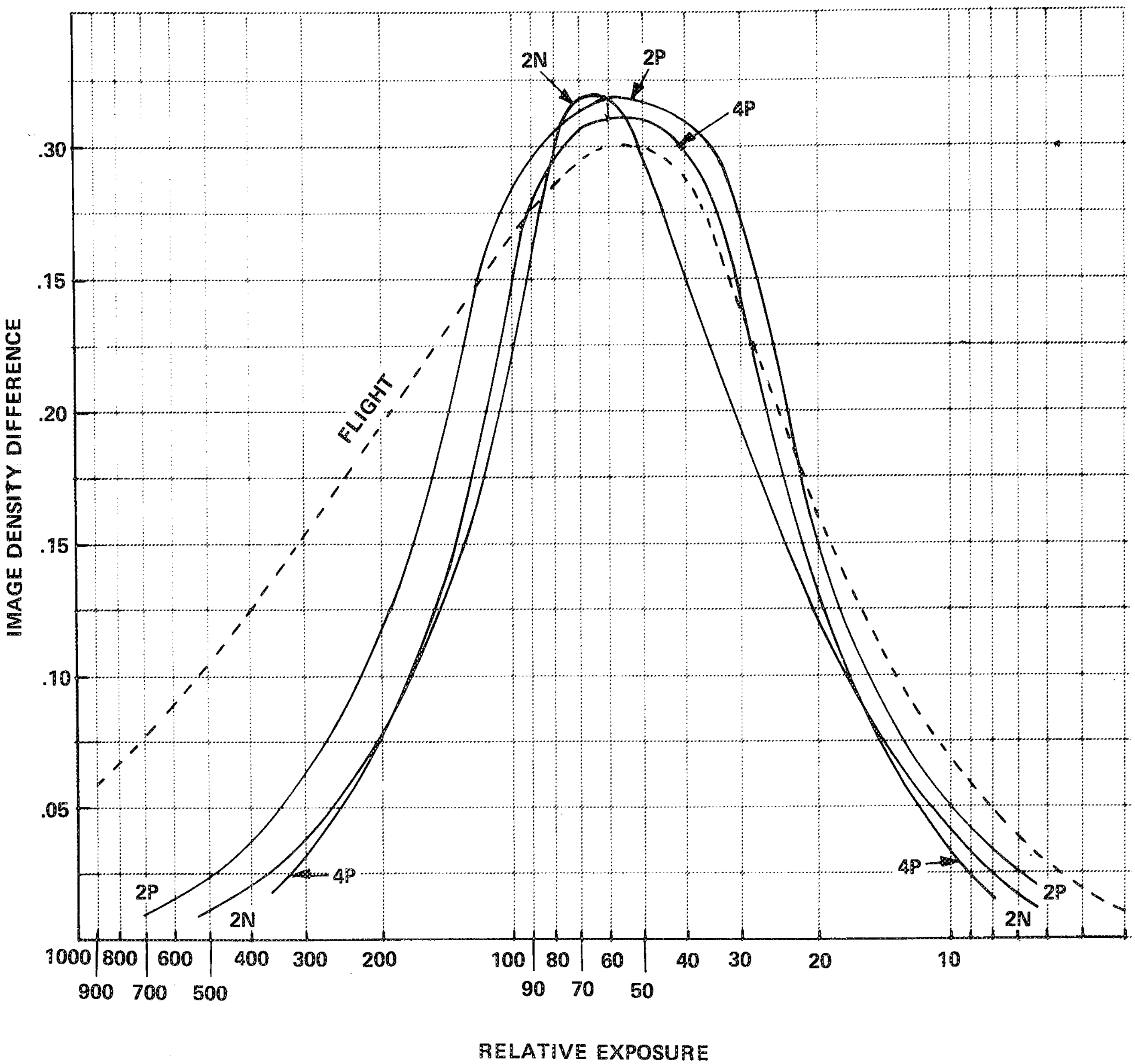

Figure 33 PAN CAMERA CONTRAST REPRODUCTION

density difference than any of the subsequent copies. A loss in contrast of about 0.7 density units occurs. In the case of the metric camera photography (Figure 32) a similar effect occurs in the bright lunar surface areas except for the master positive copy which shows some enhancement in the contrast. It is worthwhile to note that both sets of imagery also show some loss of apparent contrast in the low exposure or dark surface regions.

From these results it is concluded that one potential source of information loss between the original flight film and subsequent copies is the compression introduced by the Huter-Driffield response curve of the copying processes. One method for correcting this situation would be to alter the chemical processing to lower gamma and increase the dynamic range or employ another reproduction film. The technique of using a lower gamma will cause some loss of contrast for mid-exposure targets. The extreme density values recorded on the flight film should be returned over a reduced portion of the linear region of the response curve, say about 2/3. This would insure that the density differences on the high exposure (bright areas) and low exposure (dark areas) of the lunar surface would not suffer further compression due to the toe and shoulder of the copy response functions.

5. CONCLUSIONS

The use of image evaluation methods for assessing the detail content of Apollo orbital photography has been demonstrated. Edge analyses using shadow-to-sunlight edges interior to craters were successfully used to evaluate residual motion smear present in Apollo 8 photography and to evaluate possible loss of fine detail in the reproduction of Apollo 15 imagery. In the case of Apollo 12 and 14 imagery high solar evaluation angles prevented the successful application of edge analyses methods although a bright ray present in several frames of Apollo 14 imagery yielded limited success.

NBS charts which were exposed onto the leader of the flight film for the Apollo 8, 12 and 14 missions were successfully used to establish baseline performance and to evaluate possible loss of fine detail during image reproduction.

The analyses of motion compensation of the Apollo 8 bracket-mounted Hasselblad imagery using the Command Module attitude control system showed about 30% compensation increasing the ground resolution from 27 meters to better than 20 meters.

The evaluation of the loss in fine detail during reproduction of the Apollo 8, 12 and 15 imagery show no significant differences between the modulation transfer function (MTF) of the original flight film and that of the copies.

Comparison of the Apollo 8 to the Apollo 12 baseline performance for the 80mm lens indicate that the Apollo 12 imagery lost fine detail content; partially attributed to a change from EK 3400 to SO-164 for the flight film.

Comparison of the sensitometric calibration of the Apollo 15 flight film to that of the copies revealed that a loss in contrast quality occurred in the bright and dark lunar surface areas introduced by the compression of the toe and shoulder of the Hurter-Driffield response curve. Modified procedures can be introduced into the reproduction process to minimize this loss in detail content.

The success of image evaluation methods in the assessment of Apollo orbital photography suggests that NASA should continue to develop the methods for application to future manned and unmanned spacecraft involved in planetary or earth exploration.

REFERENCES

1. Kinzly, R. E.,; Mazurowski, M. J.; and Holladay, T. M.; Image Evaluation and Its Application to Lunar Orbiter. Applied Optics, Vol. 7, No. 8, August 1968, p. 1577.

2. Coltman, J. W.: The Specification of Imaging Properties by Response to a Sine Wave Input. J. Opt. Soc. Am., Vol. 44, No. 6, June 1954, p. 468.

3. Charman, W. N.: Spatial Frequency Spectra and Other Properties of Conventional Resolution Targets. Photo. Scie. Eng., Vol. 8, No. 8, September-October 1964, p. 253.

4. Mazurowski, M. J. and Kinzly, R. E.: The Precision of Edge Analysis Applied to the Evaluation of Motion-Degraded Images. Evaluation of Motion-Degraded Images, NASA SP-193, 1969, p. 11.

5. Roetling, R. G., Haas, R. C., and Kinzly, R. E.: Some Practical Aspects of Measurement and Restoration of Motion-Degraded Images. Evaluation of Motion-Degraded Images, NASA SP-193, 1969, p. 167.

6. Kinzly, R. E.; Roetling, P. G.; and Holladay, T. M.: Project SLOPE, Study of Lunar Orbiter Photographic Evaluation. NASA CR-66158, Cornell Aeronautical Laboratory, Inc., 20 May 1966.